
How Fast Should a Model Commit to Supervision? Training Reasoning Models on the J_Q Loss Continuum

Chu-Cheng Lin Eugene Ie
Google
{kitsing, eugeneie}@google.com

Abstract

SFT-then-RLVR is widely used for post-training reasoning models, but why this specific ordering, and why RLVR-only stalls at cold start, have lacked a unifying theoretical account. We provide that account under a unified loss family J_Q using the Tsallis q -logarithm. J_Q is a single-parameter family that interpolates between RLVR (at $q=0$, the *exploitation pole*) and the log-marginal-likelihood over latent trajectories (at $q=1$, the *density-estimation pole*), under which the standard pipeline corresponds to a stepwise $q=1 \rightarrow 0$ schedule. All members share the same per-example gradient direction, differing only by a per-instance amplification P_θ^{-q} that reweights each instance independently of the learning rate. Under gradient flow analysis, we show that the exploitation pole requires $\Omega(1/p_0)$ time to escape cold start but is robust to label noise, while the density-estimation pole escapes in $\Theta(\log(1/p_0))$ but memorizes label noise. This separation explains how SFT ($q=1$) first moves the model out of the cold-start regime, followed by the more robust RLVR ($q=0$), under the SFT-then-RLVR paradigm. We further derive two Monte Carlo estimators that directly optimize fixed- q on the J_Q continuum, without annotated rationales: Gradient-Amplified RL (GARL) and Posterior-Attenuated Fine-Tuning (PAFT), with shared bias $O(q/MP_\theta^q)$ but different variance and stability properties. On FinQA, HotPotQA, and MuSiQue, GARL at sufficiently high q substantially mitigates cold-start stalling, escaping cold start where GRPO fails entirely. In warm start, GARL at low q dominates FinQA where training is stable; on HotPotQA and MuSiQue, GARL destabilizes and PAFT at $q=0.75$ remains stable, reaching 47.9 m@16 on HotPotQA (+13.9 over GRPO).

1 Introduction

The standard recipe for adapting reasoning models is supervised fine-tuning (SFT) on annotated rationales followed by reinforcement learning from verifiable rewards (RLVR) [Ouyang et al., 2022, DeepSeek-AI, 2025, Shao et al., 2024, Chu et al., 2025]. Yet two questions about it lack a unifying theoretical account: *why this specific ordering* and *why RLVR alone stalls at cold start* (when initial P_θ is near zero). Recent Rao–Blackwellized variants [Zhou et al., 2026] ensure non-zero gradients but, as we show, reduce variance without accelerating escape.

We provide such an account under exact-match supervision. Using the Tsallis q -logarithm [Tsallis, 1988], we define a loss continuum J_Q with a scalar *commitment* parameter $q \in [0, 1]$ that interpolates between REINFORCE-style exploitation and log-marginal-likelihood maximization. All members of J_Q share one per-instance gradient direction, differing only by a factor P_θ^{-q} (Figure 1; formal definitions in Section 2). This per-instance reweighting amplifies the gradient on unfamiliar (low- P_θ) instances when q is large — an effect no global learning rate can replicate.¹

¹Adam-style adaptive optimizers [Kingma and Ba, 2014] adjust step sizes per-*parameter*, not per-*example*; they cannot substitute for P_θ^{-q} .

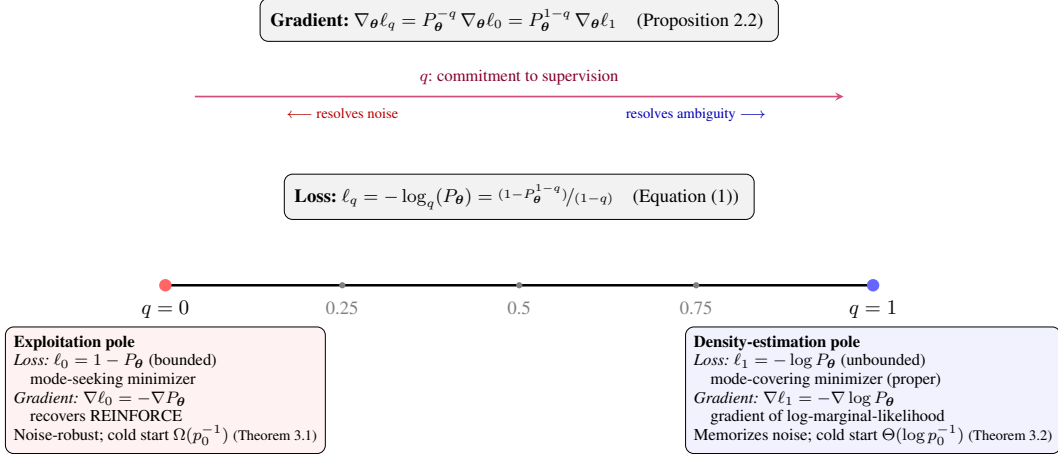


Figure 1: The J_Q loss family is a continuum between exploitation ($q = 0$) and density estimation ($q = 1$) losses (poles at either end of the axis below); correspondingly, commitment is the induced gradient amplification (P_θ^{-q} ; top arrow). High q resolves ambiguity (fast cold-start escape) but also memorizes noise; low q resolves noise (robust filtering) but cannot escape cold start. p_0 denotes initial success probability; convergence results assume bounded score (Section 3).

The commitment q thus acts as a training-time analog of inference temperature: high q enables fast cold-start escape in $\Theta(\log(1/p_0))$ time (Theorem 3.2) but memorizes label errors (Proposition D.2); low q is noise-robust but escape slows to $\Omega(1/p_0)$ (Theorem 3.1). This explains why SFT-then-RLVR succeeds: SFT corresponds to $q=1$ (log-marginal-likelihood maximization with the annotated rationale fixed), where P_θ^{-1} amplification escapes cold start; switching to RLVR ($q=0$) afterward filters noisy supervision. It also suggests that an intermediate q can cold-start a reasoning model under J_Q directly, without SFT. Since P_θ is intractable, we estimate $\nabla_\theta J_Q$ by two Monte Carlo factorizations with different stability (Section 4).

Contributions. (1) **The J_Q loss family** (Sections 2 to 3). J_Q interpolates between a bounded, noise-robust loss at $q=0$ and an unbounded, mode-covering loss at $q=1$. Its categorical minimizer is the escort $\theta_j^* \propto \alpha_j^{1/q}$ (Theorem 2.1); J_Q also enforces a dispersion penalty across examples (Proposition C.1). The shared P_θ^{-q} amplification separates escape speed: $\Omega(1/p_0)$ at $q=0$ vs. $\Theta(\log 1/p_0)$ at $q=1$ (Theorems 3.1 and 3.2). (2) **Two gradient estimators: GARL and PAFT** (Section 4). The dual factorization yields **Gradient-Amplified RL** (prior sampling, amplified by P_θ^{-q} ; generalizes RB-REINFORCE [$q=0$; Zhou et al., 2026] and IWAE [$q=1$; Burda et al., 2015]) and **Posterior-Attenuated Fine-Tuning** (posterior resampling, attenuated by P_θ^{1-q} ; generalizes the EM gradient update [$q=1$; Dempster et al., 1977, Phan et al., 2023]). Both have bias $O(q/MP_\theta^q)$; GARL has lower variance, but PAFT remains stable in warm start where GARL destabilizes on HotPotQA and MuSiQue (Section 5). (3) **Empirical validation** (Section 5). On FinQA, HotPotQA, and MuSiQue with exact-match training rewards: cold-start GARL at sufficiently high q escapes where GRPO fails entirely for both 0.6B and 8B models. In warm start, the best stable method beats GRPO by +7.0 to +13.9 maj@16: GARL ($q=0.25$) on FinQA (38.7 vs. 27.8) where training is stable; PAFT ($q=0.75$) on HotPotQA (47.9 vs. 34.0, where GARL collapses at all tested q) and MuSiQue (22.4 vs. 15.4, where GARL’s higher peak does not survive training).

2 Setup and the J_Q Loss Family

We consider supervised conditional generation with latent reasoning trajectories: an autoregressive language model p_θ with parameters $\theta \in \mathbb{R}^d$, trained on a dataset \mathcal{D} of input-output pairs $(\mathbf{x}^*, \mathbf{y}^*)$. Given input \mathbf{x} , the model samples an unannotated latent rationale \mathbf{z} from $p_\theta(\cdot | \mathbf{x})$ then an output $\hat{\mathbf{y}} \sim p_\theta(\cdot | \mathbf{x}, \mathbf{z})$, inducing the marginal $p_\theta(\mathbf{y} | \mathbf{x}) = \sum_{\mathbf{z}} p_\theta(\mathbf{z}, \mathbf{y} | \mathbf{x})$. The latent \mathbf{z} may be a chain of thought [Wei et al., 2022], proof trace, program, etc.; we treat it as an *operational* latent mediating the output distribution.

Success probability and endpoint losses. For each supervised example, the **success probability** is $P_\theta \triangleq p_\theta(\mathbf{y}^* | \mathbf{x}^*)$. We define the **exploitation loss** $J_0(\theta) \triangleq \mathbb{E}_{\mathcal{D}}[1 - P_\theta]$ and **density-estimation loss** $J_1(\theta) \triangleq \mathbb{E}_{\mathcal{D}}[-\log P_\theta]$, both minimized at $P_\theta = 1$. Under exact-match supervision $R(\hat{\mathbf{y}}, \mathbf{y}^*) = \mathbb{I}(\hat{\mathbf{y}} = \mathbf{y}^*)$, $J_0 = 1 - \mathbb{E}_{\mathcal{D}}[\text{reward}]$ (Proposition B.1), so minimizing J_0 maximizes expected reward.

The J_Q family. The Tsallis q -logarithm [Tsallis, 1988], $\log_q(u) = (u^{1-q} - 1)/(1-q)$ for $u \in (0, 1]$ with $\log_1(u) \triangleq \log u$, defines the per-example loss and dataset objective

$$\ell_q(\theta; \mathbf{x}^*, \mathbf{y}^*) \triangleq -\log_q P_\theta = \frac{1 - P_\theta^{1-q}}{1-q}, \quad J_Q(\theta, q) = \mathbb{E}_{(\mathbf{x}^*, \mathbf{y}^*) \sim \mathcal{D}}[\ell_q(\theta; \mathbf{x}^*, \mathbf{y}^*)], \quad (1)$$

recovering $J_Q(\theta, 0) = J_0$ and $J_Q(\theta, 1) = J_1$. At $q < 1$ the per-example loss is bounded and noise-robust; at $q = 1$ it is unbounded and the model fits the training distribution exactly, including label errors. Strict convexity of $-\log_q$ for $q > 0$ gives $J_Q \geq -\log_q(\mathbb{E}_{\mathcal{D}}[P_\theta])$: J_Q penalizes non-uniform success across examples (*dispersion penalty*, Proposition C.1). Moreover, higher- q also penalizes non-uniformness on the prediction, which we formalize next.

q as a training-time temperature. Just as inference temperature controls output spread at decoding time, q controls it at training time: ℓ_q penalizes non-uniform θ more when q increases. To illustrate this point, we consider K -category models with empirical frequencies $\alpha_j > 0$. J_Q 's minimizer for such models is the **escort distribution** [Beck and Schlögl, 1993] of order $1/q$:

Theorem 2.1. [Minimizers of J_Q in the categorical model] For $q \in (0, 1]$, the unique minimizer of $J_Q(\theta, q) = \sum_j \alpha_j (-\log_q \theta_j)$ over $\theta \in \Delta_K$ is $\theta_j^*(q) = \frac{\alpha_j^{1/q}}{\sum_k \alpha_k^{1/q}}$. For $q = 0$, any vertex e_j with $j \in \operatorname{argmax}_k \alpha_k$ is optimal.

Proof sketch. Strict convexity for $q > 0$ ensures uniqueness; Lagrange multipliers yield $\theta_k \propto \alpha_k^{1/q}$ (full proof in Section C). \square

The escort interpolates continuously from full coverage ($q=1: \theta^* = \alpha$) to pure mode-seeking ($q \rightarrow 0$), with $q=1$ the unique strictly proper scoring rule in J_Q (Corollary C.3).

Gradient geometry. All members of J_Q share one per-example gradient direction, factoring through either the exploitation loss endpoint $\nabla_\theta \ell_0$ or the density-estimation loss endpoint $\nabla_\theta \ell_1$:

Proposition 2.2 (Gradient geometry and dual factorization). For any fixed supervised example $(\mathbf{x}^*, \mathbf{y}^*)$ with $P_\theta > 0$ and any $q \in [0, 1]$,

$$\nabla_\theta \ell_q(\theta; \mathbf{x}^*, \mathbf{y}^*) = \underbrace{P_\theta^{-q}}_{\text{amplify}} \nabla_\theta \ell_0(\theta; \mathbf{x}^*, \mathbf{y}^*) = \underbrace{P_\theta^{1-q}}_{\text{attenuate}} \nabla_\theta \ell_1(\theta; \mathbf{x}^*, \mathbf{y}^*). \quad (2)$$

Proof. By the chain rule and $\frac{d}{du} \log_q(u) = u^{-q}$: $\nabla_\theta \ell_q = -P_\theta^{-q} \nabla_\theta P_\theta = P_\theta^{-q} \nabla_\theta \ell_0$. Since $\nabla_\theta \ell_0 = -\nabla_\theta P_\theta = P_\theta \nabla_\theta \ell_1$, the second equality follows. \square

The amplification $P_\theta^{-q} \in [1, \infty)$ controls both cold-start escape speed (Section 3) and ratio-estimator bias (Section 4); the RL factorization motivates GARL (Section 4.1), the FT factorization motivates PAFT (Section 4.2).

3 Commitment Dynamics under Gradient Flow

Under gradient flow, escape from a cold start ($p_0 = P_{\theta(0)} \ll 1$) takes $\Omega(1/p_0)$ time at the exploitation pole ($q=0$) but only $\Theta(\log(1/p_0))$ at the density-estimation pole ($q=1$). This exponential separation in $1/p_0$ is governed by the amplification factor P_θ^{-q} and the dynamics $\dot{p} = p^{2-q} \|s(\theta)\|^2$. Our analysis is stylized: it tracks single-example success probability under continuous-time gradient flow, isolating the role of the amplification factor rather than fully modeling multi-example LM optimization.

Dynamics of the success probability. We study gradient flow $\dot{\theta} = -\nabla_{\theta} \ell(\theta)$ [Su et al., 2016], which isolates closed-form rates from step-size effects without requiring convexity ($\dot{p} \geq 0$ always). For a single example with score $s(\theta) \triangleq \nabla_{\theta} \log P_{\theta}$, Proposition 2.2 gives

$$\dot{p} = \nabla_{\theta} P_{\theta} \cdot \dot{\theta} = P_{\theta}^{-q} \|\nabla_{\theta} P_{\theta}\|^2 = p^{2-q} \|s(\theta)\|^2, \quad (3)$$

where q 's entire effect on convergence is captured by the exponent $2 - q$ ($\|s\|^2$ is q -independent).

Why q matters at cold start. For $p_0 \triangleq p(0) \ll 1$ and approximately constant $\|s\|$, the time to reach target δ is $T \sim \int_{p_0}^{\delta} u^{-(2-q)} du$. The exponent $2 - q$ sets the divergence rate as $p_0 \rightarrow 0$: at $q = 0$, $\int u^{-2} du \sim p_0^{-1}$; at $q = 1$, $\int u^{-1} du \sim \log(1/p_0)$.

Cold-start escape rates. We present the separation in two results: an $\Omega(\cdot)$ bound assuming that score is upper-bounded (training with low- q is *provably slow*), then a matching $\Theta(\cdot)$ rate assuming that the score is also lower-bounded.

Theorem 3.1. [Exploitation is provably slow] Let $\theta \in \mathbb{R}^d$ parameterize any differentiable model. Consider gradient flow on $\ell_q(\theta) = -\log_q(P_{\theta})$, starting from $p_0 = P_{\theta(0)} \in (0, 1/2)$ with fixed target $\delta \in (p_0, 1/2]$. Suppose $\|s(\theta(t))\| \leq C \in \mathbb{R}$. Then as $p_0 \rightarrow 0$:

$$T_q(p_0, \delta) = \Omega\left(\frac{p_0^{-(1-q)}}{1-q}\right) \text{ for } q \in [0, 1),$$

$$T_1(p_0, \delta) = \Omega\left(\log \frac{1}{p_0}\right).$$

Proof sketch. From $\dot{p} = p^{2-q} \|s\|^2 \leq C^2 p^{2-q}$, the success probability grows no faster than $C^2 p^{2-q}$. Integrating: $T_q \geq \frac{1}{C^2} \int_{p_0}^{\delta} u^{-(2-q)} du$, which evaluates to $\Omega(p_0^{-(1-q)}/(1-q))$. \square

$\|s\| \leq C$ is a common regularity assumption (verified in closed form for the scalar sigmoid in Section D.1); the exploitation pole thus has escape time $\Omega(1/p_0)$ under this assumption.

Theorem 3.2. [Tight cold-start escape rates] Under the same setup as Theorem 3.1, suppose additionally that $\|s(\theta(t))\| \geq c > 0$ throughout the trajectory. Then as $p_0 \rightarrow 0$,

$$T_q(p_0, \delta) = \Theta\left(\frac{p_0^{-(1-q)}}{1-q}\right) \text{ for } q \in [0, 1), \quad T_1(p_0, \delta) = \Theta\left(\log \frac{1}{p_0}\right),$$

and consequently $T_q(p_0, \delta)/T_{q'}(p_0, \delta) \rightarrow \infty$ for any $q < q' \leq 1$.

The lower bound $\dot{p} \geq c^2 p^{2-q}$ gives the matching upper bound via the same integration (Section D). The q -dependent separation comes from the assumption-free factor p^{2-q} in Equation (3), so the pole ordering persists even where $\|s\| \geq c$ fails; exact rates for a sigmoid model are in Section D.1. Restricting the target to $\delta \leq 1/2$ keeps the trajectory away from $p \rightarrow 1$ where the score naturally vanishes for softmax parameterizations.

Noise fitting is symmetric. The same machinery gives an exact dual: under the canonical sigmoid model, growing noise contamination from \tilde{p}_0 to a fixed target takes $T_q^{\text{noise}}(\tilde{p}_0) = \Theta(\tilde{p}_0^{-(1-q)}/((1-q)\epsilon))$ for $q \in (0, 1)$ and $\Theta(\log(1/\tilde{p}_0)/\epsilon)$ at $q=1$ (Proposition D.2 in Section D.5, diverging at $q=0$) — matching cold-start escape's exponent in the small starting probability, with ϵ the only additional rate factor. So P_{θ}^{-q} accelerates clean and corrupted commitment by the same factor, and SFT-then-RL [Ouyang et al., 2022, DeepSeek-AI, 2025, Chu et al., 2025] becomes a hard $q=1 \rightarrow q=0$ switch: SFT escapes cold start via P_{θ}^{-1} amplification; RL afterwards halts noise commitment ($T_q^{\text{noise}} \rightarrow \infty$ at $q=0$). The reverse order gets neither; J_Q replaces the hard switch with a smooth interpolation.

4 Gradient Estimators for J_Q

The marginal $P_{\theta} = \sum_{\mathbf{z} \in \mathcal{Z}} p_{\theta}(\mathbf{z}, \mathbf{y}^* | \mathbf{x}^*)$ in $\nabla_{\theta} \ell_q$ is intractable, so we estimate the gradient by Monte Carlo. The dual factorization (Proposition 2.2) yields two natural estimators:

- **GARL** (Section 4.1): sample from the prior $p_\theta(\mathbf{z} \mid \mathbf{x}^*)$, estimate $\nabla_\theta \ell_0$ and P_θ from the same samples, amplify by $(\bar{w}_M)^{-q}$ (a plug-in estimator of the amplification factor P_θ^{-q}).
- **PAFT** (Section 4.2): approximately sample from the posterior $p_\theta(\mathbf{z} \mid \mathbf{x}^*, \mathbf{y}^*)$, estimate $\nabla_\theta \ell_1$ via teacher forcing, attenuate by $(\bar{w}_M)^{1-q}$ (estimating P_θ^{1-q}).

Drop-in compute cost. Both estimators are drop-in replacements for RB-REINFORCE/RLOO at the same rollout budget: GARL adds an $O(M)$ scalar reweighting on top of RB-RLOO [Zhou et al., 2026], and PAFT adds one categorical resample over the prior weights followed by teacher forcing on already-generated tokens. Neither requires extra forward passes.

4.1 GARL: Gradient-Amplified RL

A plug-in Monte Carlo estimator. Fix a supervised example $(\mathbf{x}^*, \mathbf{y}^*)$ and draw M i.i.d. latent trajectories $\mathbf{z}^{(1)}, \dots, \mathbf{z}^{(M)} \sim p_\theta(\cdot \mid \mathbf{x}^*)$. Define the per-sample likelihood weight and gradient contribution:

$$w_m \triangleq p_\theta(\mathbf{y}^* \mid \mathbf{x}^*, \mathbf{z}^{(m)}), \quad g_m \triangleq -w_m \nabla_\theta \log p_\theta(\mathbf{z}^{(m)}, \mathbf{y}^* \mid \mathbf{x}^*), \quad (4)$$

with empirical means $\bar{w}_M \triangleq \frac{1}{M} \sum_m w_m$ and $\bar{g}_M \triangleq \frac{1}{M} \sum_m g_m$. By the log-trick,

$$\mathbb{E}[\bar{w}_M] = P_\theta, \quad \mathbb{E}[\bar{g}_M] = -\sum_{\mathbf{z}} \nabla_\theta p_\theta(\mathbf{z}, \mathbf{y}^* \mid \mathbf{x}^*) = -\nabla_\theta P_\theta = \nabla_\theta \ell_0. \quad (5)$$

Plugging these into the RL factorization of Proposition 2.2 yields the plug-in estimator

$$\hat{\nabla}_\theta \ell_q(q, \theta; \mathbf{x}^*, \mathbf{y}^*, M) \triangleq \frac{\bar{g}_M}{(\bar{w}_M)^q}. \quad (6)$$

The dataset-level estimator of $\nabla_\theta J_Q$ averages Equation (6) over a minibatch: GARL amplifies the RL gradient \bar{g}_M by the plug-in estimate $(\bar{w}_M)^{-q}$ of P_θ^{-q} . At the endpoints, GARL recovers RB-REINFORCE [$q=0$; Zhou et al., 2026] and the IWAE gradient estimator [$q=1$; Burda et al., 2015]; see Section E.2.

Update normalization. The per-sample weight $w_m/(\bar{w}_M)^q$ (the effective reward under the RL view) has maximum M^q , so the centered advantage c_m in Equation (17) can range up to M^q in magnitude. To keep the per-sample advantage uniformly bounded as q varies, the algorithms Algorithms 1 and 2 divide by M^q , yielding $c_m/M^q \in [-1, 1]$. The mathematical estimators Equations (9) and (17) target $\nabla_\theta \ell_q$ directly; the algorithm-side $1/M^q$ is equivalent to applying a q -independent learning rate to the bounded-advantage form (vs. a q -dependent learning rate to the unscaled form).

Consistency and finite-sample bias. Equation (6) is a ratio estimator: it reuses the same samples in numerator and denominator, so it is biased at finite M even though \bar{w}_M and \bar{g}_M are individually unbiased.²

Theorem 4.1. [Consistency and bias expansion] Fix a supervised example $(\mathbf{x}^*, \mathbf{y}^*)$ and assume:

1. $P_\theta > 0$;
2. $\mathbb{E}[\|g_m\|^2] < \infty$;
3. $w_m \geq \epsilon$ a.s. for some $\epsilon > 0$.

Then for any fixed $q \in [0, 1]$, the estimator is consistent: $\hat{\nabla}_\theta \ell_q \xrightarrow{a.s.} \nabla_\theta \ell_q$ as $M \rightarrow \infty$. Moreover, the leading-order bias is

$$\mathbb{E}[\hat{\nabla}_\theta \ell_q] - \nabla_\theta \ell_q = \frac{q}{MP_\theta^{q+1}} \left[\frac{q+1}{2} \nabla_\theta \ell_1 \mathbf{Var}(w_m) - \mathbf{Cov}(g_m, w_m) \right] + O(M^{-2}) \quad \text{as } M \rightarrow \infty. \quad (7)$$

Under additionally bounded marginal and per-trajectory scores ($\|\nabla_\theta \log P_\theta\| \leq C$, $\|\nabla_\theta \log p_\theta(\mathbf{z}, \mathbf{y}^* \mid \mathbf{x}^*)\| \leq C'$), the bracketed term is $O(P_\theta)$, so the bias simplifies to $O(q/MP_\theta^q)$.

²Assumptions 1–2 are standard regularity. Assumption 3 controls the ratio-estimator denominator at fixed θ : for autoregressive softmax models, $w_m = \prod_{t=1}^T p_\theta(y_t^* \mid \cdot) \geq \epsilon_0^T$ for some $\epsilon_0 > 0$. The bound is not uniform over training, and may also shrink as $P_\theta \rightarrow 0$.

At $q=0$ the bias vanishes *exactly* for all M : the estimator reduces to the unbiased sample mean \bar{g}_M (Equation (5)). The proof is a delta-method expansion of \bar{g}_M/\bar{w}_M^q around $(P_\theta, \nabla \ell_0)$ (Section E). The J_Q -specific feature is the joint dependence on q and P_θ : the same P_θ^{-q} that enables fast escape (Theorems 3.1 and 3.2) degrades estimator quality at the same rate, predicting that intermediate q outperforms both endpoints—confirmed in Section 5. The expansion is a fixed- P_θ , large- M asymptotic; in cold start it identifies the direction of degradation, not a uniform bound.

Control variate. We apply the standard leave-one-out control variate [Kool et al., 2019] to GARL’s score-function term, centering the per-sample coefficient $w_m/(\bar{w}_M)^q$ against $(\bar{w}_{-m})^{1-q}$ where $\bar{w}_{-m} \triangleq \frac{1}{M-1} \sum_{j \neq m} w_j$ (full RLOO estimator and derivation in Section E.1). The control variate preserves the bias of Theorem 4.1 (Proposition E.1). At $q = 0$ this recovers the Rao–Blackwellized RLOO of Zhou et al. [2026]; at $q = 1$ the centered weight becomes $w_m/\bar{w}_M - 1$, a self-normalizing baseline. Pseudocode is in Algorithm 1.

4.2 PAFT: Posterior-Attenuated Fine-Tuning

GARL samples from the prior and amplifies by P_θ^{-q} —sometimes massively. The FT factorization (Equation (2)) offers an alternative: sample from the posterior $p_\theta(\mathbf{z} \mid \mathbf{x}^*, \mathbf{y}^*)$ —where rationales already agree with \mathbf{y}^* —and attenuate by $P_\theta^{1-q} \in [0, 1]$.

Posterior form of the gradient. Expanding $\nabla_\theta \ell_1 = -\nabla_\theta \log P_\theta$ as a posterior expectation:

$$\nabla_\theta \ell_q = -P_\theta^{1-q} \cdot \mathbb{E}_{\mathbf{z} \sim p_\theta(\mathbf{z} \mid \mathbf{x}^*, \mathbf{y}^*)} [\nabla_\theta \log p_\theta(\mathbf{z}, \mathbf{y}^* \mid \mathbf{x}^*)]. \quad (8)$$

Each sample gradient is standard SFT (teacher forcing) on a *semantically coherent* (input, rationale, answer) triple: the rationale is posterior-weighted toward agreement with \mathbf{y}^* .

Approximate posterior sampling. The posterior is intractable for autoregressive models. We use importance resampling [IR; Rubin, 1988], which reuses GARL’s pool and weights: resample K indices $r_1, \dots, r_K \in \{1, \dots, M\}$ with replacement, with r_k drawn proportional to w_{r_k} . The PAFT estimator is

$$\hat{\nabla}_{\text{PAFT}} = -(\bar{w}_M)^{1-q} \cdot \frac{1}{K} \sum_{k=1}^K \nabla_\theta \log p_\theta(\mathbf{z}^{(r_k)}, \mathbf{y}^* \mid \mathbf{x}^*). \quad (9)$$

At $q = 1$, the attenuation vanishes ($(\bar{w}_M)^{1-q} = 1$) and PAFT recovers the EM gradient update—the M -step gradient evaluated over E-step posterior samples [Dempster et al., 1977, Phan et al., 2023]; Section E.2 lists all endpoint reductions.

Bias and variance. Importance resampling preserves the gradient mean: PAFT inherits GARL’s leading bias expansion (Proposition E.3), which under the bounded-score conditions of Theorem 4.1 simplifies to $O(q/M P_\theta^q)$, and has strictly higher variance by the law of total variance (Proposition E.4; full derivations in Section E.3).

Yet PAFT can produce better training dynamics: GARL’s lower variance comes from mixing bad rationales with small weights, while PAFT excludes them before the gradient is formed. Posterior-resampling noise preserves the FT endpoint’s semantic coherence, making PAFT more stable at warm start despite higher variance (Section 5); see Algorithm 2.

5 Empirical Validation

We validate the theoretical predictions and empirical effectiveness of GARL and PAFT on three reasoning benchmarks—FinQA [Chen et al., 2021], HotPotQA [Yang et al., 2018], and MuSiQue [Trivedi et al., 2022]—using post-trained Qwen 3 0.6B and 8B models [Yang et al., 2025] under both cold-start and warm-start conditions.

Table 1: Cold-start results across 3 benchmarks \times 2 scales (Qwen 3; [Yang et al., 2025]). At 0.6B, GRPO and GARL with $q \leq 0.5$ fail entirely on every benchmark; only $q \geq 0.75$ escapes, with $q=0.75$ outperforming $q=1$ on p@1. At 8B, the threshold shifts to $q \geq 0.85$, and the cold-start ordering replicates qualitatively. Warm-start prompted GRPO baselines are included as a cross-regime reference: cold-start GARL at $q \in \{0.75, 0.85\}$ exceeds them on every metric across all three benchmarks (a confounded comparison: see body discussion). Best per scale \times benchmark \times metric in bold. For Qwen 3 0.6B GRPO (warm) and GARL $q=0.75$ results, we report mean and standard deviation over 3 different seeds. Note: FinQA’s 8B GRPO (warm) m@16 inverts the scale ordering ($19.6 < 27.8$ at 0.6B), while HotPotQA and MuSiQue scale as expected; 8B numbers are single-seed.

Method	FinQA			HotPotQA			MuSiQue		
	p@1	p@16	m@16	p@1	p@16	m@16	p@1	p@16	m@16
<i>Qwen 3 0.6B (cold-start)</i>									
GRPO	0	0	0	0	0	0	0	0	0
GRPO (warm)	20.6 \pm 2.0	48.5 \pm 0.7	27.8 \pm 1.1	29.6 \pm 0.6	56.8 \pm 1.6	34.0 \pm 0.7	12.9 \pm 1.2	35.7 \pm 1.9	15.4 \pm 0.4
GARL $q=0$ (RB-RLOO)	0	0	0	0	0	0	0	0	0
GARL $q=0.25$	0	0	0	0	0	0	0	0	0
GARL $q=0.5$	0	0	0	0	0	0	0	0	0
GARL $q=0.75$	30.5 \pm 0.3	61.1 \pm 0.5	38.6 \pm 0.6	53.4 \pm 0.6	74.1 \pm 1.0	57.4 \pm 0.9	27.5 \pm 0.9	58.2 \pm 0.7	35.6 \pm 1.5
GARL $q=1$	21.9	58.7	33.5	48.7	75.5	56.6	21.6	58.1	32.5
<i>Qwen 3 8B (cold-start)</i>									
GRPO	0	0	0	0	0	0	0	0	0
GRPO (warm)	18.7	26.2	19.6	34.9	50.5	39.6	26.7	51.9	31.1
GARL $q=0$	0	0	0	0	0	0	0	0	0
GARL $q=0.75$	0	0	0	0	0	0	0	0	0
GARL $q=0.85$	45.0	75.2	52.9	64.8	81.5	68.6	58.7	78.8	62.9
GARL $q=1$	38.4	75.6	50.1	61.6	81.4	67.9	57.1	79.6	64.5

5.1 Experimental setup

Our experiments operate without annotated rationales (output-level supervision only); fixed- q GARL and PAFT are first-step demonstrations of what the J_Q perspective enables, with annealing schedules over q left to future work. We organize the empirical findings around three research questions: **RQ1** — can fixed- q J_Q optimization escape cold start? **RQ2** — is J_Q optimization still useful in warm-start? **RQ3** — is PAFT empirically more stable than GARL in warm-start?

Scenarios. *Warm start* evaluates whether J_Q optimization remains useful when the model is already task-aligned — either via SFT on annotated rationales (when available) or via instruction prompting alone (when not; e.g., Wei et al., 2022, DeepSeek-AI, 2025). We use the prompting alternative: task inputs are natural-language prompts with task descriptions and answer-formatting instructions; the un-adapted model can occasionally produce correct answers, so reward is not sparse. *Cold start* uses linearized $(\mathbf{x}^*, \mathbf{y}^*)$ pairs with no task description and no formatting instructions; the model must discover both how to solve the problem and how to format the answer, and initial P_θ is very low.

Datasets, methods, and evaluation. We sample training, validation, and test subsets from Huggingface. GRPO, GARL, and PAFT all use $M = 32$ rollouts per prompt during training for Qwen 3 0.6B, and $M = 16$ for 8B. All methods use 16 samples per prompt at evaluation. GARL (Algorithm 1) uses the RLOO variance reduction (Equation (17)); PAFT (Algorithm 2) resamples $K = M$ trajectories from the same pool. We enforce per-rationale token budgets following Muennighoff et al. [2025]. We evaluate $q \in \{0, 0.25, 0.5, 0.75, 1\}$ at 0.6B, and $q \in \{0, 0.75, 0.85, 1\}$ at 8B (where the cold-start escape threshold shifts upward; Section 5.2). Training uses exact-match rewards (Section 2); evaluation uses relaxed substring match (correct if \mathbf{y}^* appears as a substring of $\hat{\mathbf{y}}$). We report p@1 (single-sample accuracy), p@ k (best-of- k , rewards coverage), and m@ k (majority vote over k samples [Wang et al., 2023]). Reported test numbers are taken from the checkpoint with highest validation m@16; unless otherwise marked with \pm , numbers are single-seed. Additional experiment setup details are in Section F.

5.2 RQ1: Can fixed- q optimization escape cold start?

Cold start tests whether commitment P_θ^{-q} determines escape from a sparse-reward regime (Theorem 3.2).

Table 2: Warm-start m@16 across three benchmarks (exact-match training rewards; evaluation uses substring match). Base = un-adapted Qwen 3 0.6B evaluated with the same prompted inputs as the trained methods. GARL at $q = 0$ recovers RB-RLOO [Zhou et al., 2026]. **GARL entries for MuSiQue and HotPotQA are peak-before-collapse** (validation accuracy collapses to zero before end of training; see Section 5.3); only FinQA GARL and all PAFT entries are steady-state. Best steady-state result per benchmark in bold: GARL at $q=0.25$ on FinQA, PAFT at $q=0.75$ on HotPotQA and MuSiQue. The best stable method beats GRPO by +7.0 to +13.9 points. For GRPO we report average m@16 numbers over 3 runs (see Table 1).

Method	FinQA	HotPotQA	MuSiQue
Base (no training, prompted)	12.6	22.2	8.9
GRPO	27.8	34.0	15.4
GARL ($q = 0$, RB-RLOO)	38.3	21.6	9.1
GARL ($q = 0.25$)	38.7	22.9	24.3
GARL ($q = 0.75$)	37.6	46.8	19.7
PAFT ($q = 0.25$)	26.6	47.0	9.0
PAFT ($q = 0.75$)	28.6	47.9	22.4

Yes, but only above a critical q that rises with model scale. GRPO, Rao–Blackwellized RLOO ($q=0$), and all $q \leq 0.5$ fail entirely on Qwen 3 0.6B; only $q \geq 0.75$ escapes. Rao–Blackwellization [Zhou et al., 2026] reduces variance but cannot accelerate escape: at $q=0$ the dynamics $\dot{p} = p^2 \|s\|^2$ have no amplification (cf. Figure 2a in Section G). The bottleneck is gradient *amplification*, not variance. The sharp transition at $q = 0.75$ matches Theorem 3.1: the lower bound $\Omega(p_0^{-(1-q)})$ grows rapidly as q decreases, so the training budget sets a critical q below which escape fails. Scaling to Qwen 3 8B [Yang et al., 2025] shifts this threshold to $q \geq 0.85$ ($q=0.75$ now fails), consistent with a lower effective initial success probability or harder optimization regime at larger scale (mechanism not directly measured). Both $q=0.75$ and $q=1$ escape at 0.6B, but $q=0.75$ achieves higher p@1 on every benchmark: the escape-vs-bias tradeoff of Theorem 4.1: $q=1$ ’s stronger amplification enables faster escape but produces higher-bias estimates. Coverage tells a subtler story: $q=1$ ’s broader mode-covering edges $q=0.75$ on HotPotQA p@16 (75.5 vs. 74.1) — extra diversity that does not survive majority voting.

Side-result: cold-start GARL is competitive with prompted warm-start GRPO. Table 1 shows GARL at $q=0.75$ (no prompts) matching or exceeding prompted warm-start GRPO on every metric across all three benchmarks, with p@1 margins of +9.9 (FinQA), +23.8 (HotPotQA), +14.6 (MuSiQue). More strikingly, it also matches or beats the best stable warm-start m@16 of Table 2 — HotPotQA 57.4 vs. PAFT’s 47.9 (+9.5); MuSiQue 35.6 vs. 22.4 (+13.2); FinQA 38.6 vs. 38.7 (tie) — despite warm-start having both prompts and training. We treat this as hypothesis-generating rather than evidence that prompts are unnecessary: cold- and warm-start runs differ in more than prompts (input formatting, output constraints, target distribution), and isolating the prompt factor needs a controlled ablation we leave to future work.

5.3 RQ2 & RQ3: Warm-start utility and PAFT vs GARL stability

Warm start tests whether GARL and PAFT help when P_θ is not negligible and standard RL already makes progress, and whether PAFT is the more stable estimator we hypothesized.³

RQ2: yes, J_Q at low q gives sizable gains over GRPO when training is stable. On FinQA, GARL is stable at all tested q , so the cost of high q — estimator bias $O(q/MP_\theta^q)$ (Theorem 4.1) and noise memorization (Proposition D.2) — outweighs its amplification benefit, and m@16 is roughly flat across $q \in [0, 0.75]$ with the best at $q=0.25$ (38.7, +10.9 over GRPO). At $q=0$ this recovers RB-RLOO of Zhou et al. [2026], which beats GRPO on FinQA (+10.5) but underperforms on HotPotQA (−12.4) and MuSiQue (−6.3): the conditional reward alone does not generalize. Raising q lifts peak accuracy on those benchmarks (HotPotQA 21.6 \rightarrow 46.8, MuSiQue 9.1 \rightarrow 19.7), but peaks do not survive training, motivating RQ3.

³All warm-start comparisons use exact-match training rewards. PAFT is not evaluated at cold start: $P_\theta^{1-q} \approx 0$ suppresses the gradient, and importance resampling suffers particle degeneracy (effective sample size ≈ 1) when all w_m are near zero.

RQ3: yes, PAFT is more stable than GARL on HotPotQA and MuSiQue. GARL on HotPotQA warm-start collapses at every q tested: validation accuracy peaks early then drops to zero before training ends (e.g., $q=0.25$: validation peaks around step 50 and reaches zero by step 100, with the best-validation checkpoint giving test m@16 of 22.9 in Table 2; $q=0.75$ follows the same pattern with test 46.8; higher q peaks higher but collapses sooner). HotPotQA exhibits broader instability — GRPO also degrades, peaking ~ 37.4 around step 100 and declining steadily to ~ 5.0 — but GARL’s collapse is qualitatively different: a sharp drop to literal zero rather than a gradual decline. PAFT shows neither pattern, reaching 47.9 m@16 on HotPotQA (best warm-start, +13.9 over GRPO) and 22.4 on MuSiQue (+7.0), and remaining stable; Figure 2b (in Section G) compares GARL and PAFT validation curves at matched $q=0.25$. We do not have a verified mechanism for the GARL-specific zero-collapse: candidate explanations include pathwise-term corruption (GARL updates $p_\theta(\mathbf{y}^* | \mathbf{x}^*, \mathbf{z})$ on every sampled \mathbf{z} , including incoherent ones; PAFT only on resampled coherent rationales) and HotPotQA-specific overfitting (also visible in GRPO). Collapse timing appears to correlate with *latent-rationale variance* $\text{Var}_{\mathbf{z}}[w(\mathbf{z})]$ under the prior, ranking FinQA (none) < MuSiQue (late) < HotPotQA (early); direct measurement and a pathwise-zeroed ablation are left to future work.

Speed vs. stability. PAFT at $q=0.25$ underperforms GRPO on MuSiQue (9.0 vs. 15.4), but its validation curve is still rising at end of training: the $P_\theta^{0.75}$ attenuation heavily down-weights hard instances, slowing learning without destabilizing it. The GARL-vs-PAFT trade-off is thus speed vs. stability — PAFT gives up per-step signal but avoids the destabilization observed in GARL on HotPotQA and MuSiQue. Raising q to 0.75 recovers speed without compromising stability: PAFT $q=0.75$ delivers the best warm-start HotPotQA result (47.9) and the honest MuSiQue recommendation (22.4 steady-state vs. GARL’s 24.3 peak-before-collapse). PAFT additionally acts as an automatic curriculum: only the easiest rationales pass the resampling filter early, broadening as P_θ grows.

6 Discussion and Future Work

The Tsallis loss continuum J_Q smooths SFT-then-RLVR into a single parameter q controlling per-instance commitment P_θ^{-q} , recovering the pipeline as a stepwise $q=1 \rightarrow q=0$ schedule and enabling training without annotated rationales via intermediate q (related work in Section A). The dual factorization (Proposition 2.2) yields complementary estimators: GARL breaches GRPO’s $\Omega(1/p_0)$ cold-start bottleneck via prior-sampling amplification; PAFT remains stable in warm start via posterior-sampling attenuation where GARL destabilizes (HotPotQA, MuSiQue).

A three-phase post-training recipe. The continuum prescribes a regime-dependent recipe: at cold start ($P_\theta \approx 0$), GARL at large q (≥ 0.75 , scaling up with model size) breaches the $\Omega(1/p_0)$ bottleneck (PAFT degenerates here); in warm start, GARL at low q where stable (FinQA), PAFT at $q \geq 0.75$ otherwise (HotPotQA, MuSiQue); as $P_\theta \rightarrow 1$, the bias shrinks and annealing $q \rightarrow 0$ recovers the unbiased RB-RLOO estimator. Validating these switches empirically is future work.

Limitations. Main experiments use Qwen 3 0.6B, three benchmarks, fixed q . The cold-start theorems are scale-agnostic and the cold-start ordering replicates at Qwen 3 8B across all three benchmarks (Section 5); the warm-start GARL collapse / PAFT stability finding is verified only at 0.6B (8B ongoing). The three-phase recipe is theory; annealed- q schedules are unvalidated. The convergence analysis is stylized (single-example, gradient flow, bounded score) and assumes exact-match supervision; general rewards are open. Future directions in Section H.

References

- Christian Beck and Friedrich Schlögl. *Thermodynamics of Chaotic Systems: An Introduction*. Cambridge Nonlinear Science Series. Cambridge University Press, 1993.
- Yuri Burda, Roger Baker Grosse, and Ruslan Salakhutdinov. Importance weighted autoencoders. volume abs/1509.00519, 2015. URL <https://api.semanticscholar.org/CorpusID:11383178>.
- Zhiyu Chen, Wenhu Chen, Charese Smiley, Sameena Shah, Iana Borova, Dylan Langdon, Reema Moussa, Matt Beane, Ting-Hao Huang, Bryan Routledge, and William Yang Wang. FinQA: A

- dataset of numerical reasoning over financial data. In Marie-Francine Moens, Xuanjing Huang, Lucia Specia, and Scott Wen-tau Yih, editors, *Proceedings of the 2021 Conference on Empirical Methods in Natural Language Processing*, pages 3697–3711, Online and Punta Cana, Dominican Republic, November 2021. Association for Computational Linguistics. doi: 10.18653/v1/2021.emnlp-main.300. URL <https://aclanthology.org/2021.emnlp-main.300/>.
- Tianzhe Chu, Yuexiang Zhai, Jihan Yang, Shengbang Tong, Saining Xie, Dale Schuurmans, Quoc V Le, Sergey Levine, and Yi Ma. SFT memorizes, RL generalizes: A comparative study of foundation model post-training. 2025. URL <https://openreview.net/forum?id=dYur3yabMj>.
- DeepSeek-AI. Deepseek-r1: Incentivizing reasoning capability in llms via reinforcement learning. 2025. URL <https://arxiv.org/abs/2501.12948>.
- AP Dempster, NM Laird, and DB Rubin. Maximum likelihood from incomplete data via the EM algorithm. *Journal of the Royal Statistical Society. Series B (Methodological)*, pages 1–38, 1977.
- Nan Ding and Radu Soricut. Cold-start reinforcement learning with softmax policy gradient. In *Proceedings of the 31st International Conference on Neural Information Processing Systems, NIPS’17*, page 2814–2823, Red Hook, NY, USA, 2017. Curran Associates Inc. ISBN 9781510860964.
- Davide Ferrari and Yuhong Yang. Maximum L_q -likelihood estimation. *The Annals of Statistics*, 38(2):753–783, 2010.
- Kelvin Guu, Panupong Pasupat, Evan Liu, and Percy Liang. From language to programs: Bridging reinforcement learning and maximum marginal likelihood. In Regina Barzilay and Min-Yen Kan, editors, *Proceedings of the 55th Annual Meeting of the Association for Computational Linguistics (Volume 1: Long Papers)*, pages 1051–1062, Vancouver, Canada, July 2017. Association for Computational Linguistics. doi: 10.18653/v1/P17-1097. URL <https://aclanthology.org/P17-1097/>.
- Diederik P. Kingma and Jimmy Ba. Adam: A method for stochastic optimization. volume abs/1412.6980, 2014. URL <https://api.semanticscholar.org/CorpusID:6628106>.
- Wouter Kool, Herke van Hoof, and Max Welling. Buy 4 REINFORCE samples, get a baseline for free! 2019. URL <https://openreview.net/forum?id=r1lgTGL5DE>.
- Kyungjae Lee, Sungjoon Choi, and Songhwai Oh. Sparse markov decision processes with causal sparse tsallis entropy regularization for reinforcement learning. *IEEE Robotics and Automation Letters*, 3(3):1466–1473, 2018. doi: 10.1109/LRA.2018.2800085.
- Sergey Levine. Reinforcement learning and control as probabilistic inference: Tutorial and review. *ArXiv*, abs/1805.00909, 2018. URL <https://api.semanticscholar.org/CorpusID:19077536>.
- Yingzhen Li and Richard E Turner. Rényi divergence variational inference. In D. Lee, M. Sugiyama, U. Luxburg, I. Guyon, and R. Garnett, editors, *Advances in Neural Information Processing Systems*, volume 29. Curran Associates, Inc., 2016. URL https://proceedings.neurips.cc/paper_files/paper/2016/file/7750ca3559e5b8e1f44210283368fc16-Paper.pdf.
- Zichen Liu, Changyu Chen, Wenjun Li, Penghui Qi, Tianyu Pang, Chao Du, Wee Sun Lee, and Min Lin. Understanding r1-zero-like training: A critical perspective. In *Second Conference on Language Modeling*, 2025. URL <https://openreview.net/forum?id=5PAF7PAY2Y>.
- Ilya Loshchilov and Frank Hutter. Decoupled weight decay regularization. In *International Conference on Learning Representations*, 2019. URL <https://openreview.net/forum?id=Bkg6RiCqY7>.
- Niklas Muennighoff, Zitong Yang, Weijia Shi, Xiang Lisa Li, Li Fei-Fei, Hannaneh Hajishirzi, Luke Zettlemoyer, Percy Liang, Emmanuel Candès, and Tatsunori Hashimoto. s1: Simple test-time scaling. In Christos Christodoulopoulos, Tanmoy Chakraborty, Carolyn Rose, and Violet Peng, editors, *Proceedings of the 2025 Conference on Empirical Methods in Natural Language Processing*, pages 20275–20321, Suzhou, China, November 2025. Association for Computational Linguistics. ISBN 979-8-89176-332-6. doi: 10.18653/v1/2025.emnlp-main.1025. URL <https://aclanthology.org/2025.emnlp-main.1025/>.

- Ofir Nachum, Yinlam Chow, and Mohammad Ghavamzadeh. Path consistency learning in tsallis entropy regularized mdps. *ArXiv*, abs/1802.03501, 2018. URL <https://api.semanticscholar.org/CorpusID:3653343>.
- Mohammad Norouzi, Samy Bengio, Zhifeng Chen, Navdeep Jaitly, Mike Schuster, Yonghui Wu, and Dale Schuurmans. Reward augmented maximum likelihood for neural structured prediction. In *Proceedings of the 30th International Conference on Neural Information Processing Systems*, NIPS’16, page 1731–1739, Red Hook, NY, USA, 2016. Curran Associates Inc. ISBN 9781510838819.
- Long Ouyang, Jeff Wu, Xu Jiang, Diogo Almeida, Carroll L. Wainwright, Pamela Mishkin, Chong Zhang, Sandhini Agarwal, Katarina Slama, Alex Ray, John Schulman, Jacob Hilton, Fraser Kelton, Luke E. Miller, Maddie Simens, Amanda Askell, Peter Welinder, Paul Francis Christiano, Jan Leike, and Ryan J. Lowe. Training language models to follow instructions with human feedback. *ArXiv*, abs/2203.02155, 2022. URL <https://api.semanticscholar.org/CorpusID:246426909>.
- Du Phan, Matthew D. Hoffman, David Dohan, Sholto Douglas, Tuan Anh Le, Aaron Parisi, Pavel Sountsov, Charles Sutton, Sharad Vikram, and Rif A. Saurous. Training chain-of-thought via latent-variable inference. In *Proceedings of the 37th International Conference on Neural Information Processing Systems*, NIPS ’23, Red Hook, NY, USA, 2023. Curran Associates Inc.
- Tom Rainforth, Adam R. Kosiorek, Tuan Anh Le, Chris J. Maddison, Maximilian Igl, Frank Wood, and Yee Whye Teh. Tighter variational bounds are not necessarily better. In *International Conference on Machine Learning (ICML)*, pages 4277–4285, 2018.
- Geoffrey Roeder, Yuhuai Wu, and David K. Duvenaud. Sticking the landing: Simple, lower-variance gradient estimators for variational inference. In *Advances in Neural Information Processing Systems (NeurIPS)*, 2017.
- Donald B. Rubin. Using the sir algorithm to simulate posterior distributions. 1988. URL <https://api.semanticscholar.org/CorpusID:115305396>.
- Zhihong Shao, Peiyi Wang, Qihao Zhu, Runxin Xu, Junxiao Song, Xiao Bi, Haowei Zhang, Mingchuan Zhang, Y.K. Li, Y. Wu, and Daya Guo. DeepSeekMath: Pushing the limits of mathematical reasoning in open language models. *arXiv preprint arXiv:2402.03300*, 2024.
- Weijie Su, Stephen Boyd, and Emmanuel J. Candès. A differential equation for modeling nesterov’s accelerated gradient method: theory and insights. *J. Mach. Learn. Res.*, 17(1):5312–5354, January 2016. ISSN 1532-4435.
- Fahim Tajwar, Guanning Zeng, Yueer Zhou, Yuda Song, Daman Arora, Yiding Jiang, Jeff Schneider, Ruslan Salakhutdinov, Haiwen Feng, and Andrea Zanette. Maximum likelihood reinforcement learning. 2026. URL <https://arxiv.org/abs/2602.02710>.
- Harsh Trivedi, Niranjan Balasubramanian, Tushar Khot, and Ashish Sabharwal. MuSiQue: Multihop questions via single-hop question composition. *Transactions of the Association for Computational Linguistics*, 2022.
- Constantino Tsallis. Possible generalization of boltzmann-gibbs statistics. *Journal of Statistical Physics*, 52:479–487, 1988. URL <https://api.semanticscholar.org/CorpusID:16385640>.
- George Tucker, Dieterich Lawson, Shixiang Gu, and Chris J. Maddison. Doubly reparameterized gradient estimators for Monte Carlo objectives. In *International Conference on Learning Representations (ICLR)*, 2019.
- Xuezhi Wang, Jason Wei, Dale Schuurmans, Quoc V Le, Ed H. Chi, Sharan Narang, Aakanksha Chowdhery, and Denny Zhou. Self-consistency improves chain of thought reasoning in language models. In *The Eleventh International Conference on Learning Representations*, 2023. URL <https://openreview.net/forum?id=1PL1NIMMrw>.
- Zecheng Wang, Deyuan Liu, Chunshan Li, Yupeng Zhang, Zhengyun Zhao, Dianhui Chu, Bingning Wang, and Dianbo Sui. Gradients must earn their influence: Unifying sft with generalized entropic objectives, 2026. URL <https://arxiv.org/abs/2602.11424>.

- Jason Wei, Xuezhi Wang, Dale Schuurmans, Maarten Bosma, Brian Ichter, Fei Xia, Ed H. Chi, Quoc V. Le, and Denny Zhou. Chain-of-thought prompting elicits reasoning in large language models. In *Proceedings of the 36th International Conference on Neural Information Processing Systems*, NIPS '22, Red Hook, NY, USA, 2022. Curran Associates Inc. ISBN 9781713871088.
- Xueru Wen, Jie Lou, Yanjiang Liu, Hongyu Lin, Ben He, Xianpei Han, Le Sun, Yaojie Lu, and Debing Zhang. Coupled variational reinforcement learning for language model general reasoning, 2026. URL <https://arxiv.org/abs/2512.12576>.
- Ronald J. Williams. Simple statistical gradient-following algorithms for connectionist reinforcement learning. *Mach. Learn.*, 8(3–4):229–256, May 1992. ISSN 0885-6125. doi: 10.1007/BF00992696. URL <https://doi.org/10.1007/BF00992696>.
- An Yang, Anfeng Li, Baosong Yang, Beichen Zhang, Binyuan Hui, Bo Zheng, Bowen Yu, Chang Gao, Chengen Huang, Chenxu Lv, Chujie Zheng, Dayiheng Liu, Fan Zhou, Fei Huang, Feng Hu, Hao Ge, Haoran Wei, Huan Lin, Jialong Tang, Jian Yang, Jianhong Tu, Jianwei Zhang, Jianxin Yang, Jiayi Yang, Jing Zhou, Jingren Zhou, Junyang Lin, Kai Dang, Keqin Bao, Kexin Yang, Le Yu, Lianghao Deng, Mei Li, Mingfeng Xue, Mingze Li, Pei Zhang, Peng Wang, Qin Zhu, Rui Men, Ruize Gao, Shixuan Liu, Shuang Luo, Tianhao Li, Tianyi Tang, Wenbiao Yin, Xingzhang Ren, Xinyu Wang, Xinyu Zhang, Xuancheng Ren, Yang Fan, Yang Su, Yichang Zhang, Yinger Zhang, Yu Wan, Yuqiong Liu, Zekun Wang, Zeyu Cui, Zhenru Zhang, Zhipeng Zhou, and Zihan Qiu. Qwen3 technical report, 2025. URL <https://arxiv.org/abs/2505.09388>.
- Zhilin Yang, Peng Qi, Saizheng Zhang, Yoshua Bengio, William W. Cohen, Ruslan Salakhutdinov, and Christopher D. Manning. HotpotQA: A dataset for diverse, explainable multi-hop question answering. In *Conference on Empirical Methods in Natural Language Processing (EMNLP)*, 2018.
- Yang Yue, Zhiqi Chen, Rui Lu, Andrew Zhao, Zhaokai Wang, Yang Yue, Shiji Song, and Gao Huang. Does reinforcement learning really incentivize reasoning capacity in LLMs beyond the base model? In *The Thirty-ninth Annual Conference on Neural Information Processing Systems*, 2025. URL <https://openreview.net/forum?id=40sgYD7em5>.
- Eric Zelikman, Yuhuai Wu, Jesse Mu, and Noah D. Goodman. Star: self-taught reasoner bootstrapping reasoning with reasoning. In *Proceedings of the 36th International Conference on Neural Information Processing Systems*, NIPS '22, Red Hook, NY, USA, 2022. Curran Associates Inc. ISBN 9781713871088.
- Zhilu Zhang and Mert R. Sabuncu. Generalized cross entropy loss for training deep neural networks with noisy labels. In *Proceedings of the 32nd International Conference on Neural Information Processing Systems*, NIPS'18, page 8792–8802, Red Hook, NY, USA, 2018. Curran Associates Inc.
- Xiangxin Zhou, Zichen Liu, Anya Sims, Haonan Wang, Tianyu Pang, Chongxuan Li, Liang Wang, Min Lin, and Chao Du. Reinforcing general reasoning without verifiers. In *The Fourteenth International Conference on Learning Representations*, 2026. URL <https://openreview.net/forum?id=nnwvwge40d>.

A Related Work

q -log losses and continua. The Tsallis q -logarithm originates in non-extensive statistical mechanics [Tsallis, 1988]; escort distributions were studied by Beck and Schlögl [1993]. Ferrari and Yang [2010] introduced maximum L_q -likelihood (MLqE), which reweights the score by $f(X; \theta)^{1-q}$, trading a small loss of asymptotic efficiency for outlier robustness; the PAFT gradient Equation (8) is the marginal-likelihood analog of this weighted score. Zhang and Sabuncu [2018] proposed generalized cross-entropy for noisy labels, an instance of the same family at the prediction level; our escort minimizer (Theorem 2.1) gives the precise mechanism. Concurrently, Wang et al. [2026] apply the deformed-log family at the *token* level for SFT; their token-level gate p^α is the single-token specialization of our example-level P_θ^{-q} , but their p is an exact softmax probability whereas P_θ is an intractable marginal. Tsallis entropy has also been used as a policy regularizer in RL [Lee et al., 2018, Nachum et al., 2018]; we use it in the loss function rather than as a policy regularizer. Tajwar et al. [2026] concurrently propose MaxRL, an RL-to-ML continuum via Maclaurin truncation of $\log p$; their estimator is unbiased for the truncated objective but exactly zero when no sample succeeds, while GARL targets the true q -loss and always has nonzero gradient since $w_m > 0$.

RL–MLE bridges and latent-variable training for reasoning. The RL-as-inference connection [Levine, 2018, Norouzi et al., 2016, Guu et al., 2017] treats MLE and RL as distinct frameworks; we embed them as endpoints of a single continuously parameterized family. Rényi variational inference [Li and Turner, 2016] provides a complementary continuum that tightens the ELBO toward $-\log P_\theta$, the target J_Q shares at $q=1$. On the latent-variable side, RLVR and GRPO [DeepSeek-AI, 2025, Shao et al., 2024] optimize expected reward; STaR [Zelikman et al., 2022] bootstraps reasoning by generating and filtering rationales; TRICE [Phan et al., 2023] and CoVRL [Wen et al., 2026] are ELBO-based variational methods at the $q=1$ pole (TRICE via MCMC-EM; CoVRL via composite prior-posterior with hybrid sampling); SPG [Ding and Soricut, 2017] samples from a reward-tilted proposal $q_\theta(\mathbf{z} | \mathbf{x}, \mathbf{y}) \propto p_\theta(\mathbf{z} | \mathbf{x}) \exp(R(\mathbf{z} | \mathbf{y}))$ for cold-start sequence-level RL, coinciding with the posterior under log-likelihood reward. At $q=1$, PAFT recovers SPG’s gradient and TRICE’s EM gradient update over posterior samples; CoVRL further hybridizes PAFT (posterior) with GARL (prior, IWAE) via composite sampling. STaR’s rejection-sampling strategy is a hard-acceptance variant of PAFT’s importance resampling (Section E.2). The J_Q continuum extends these with the $\Omega(1/p_0) \rightarrow \Theta(\log(1/p_0))$ separation across q and the dual factorization through GARL.

Gradient estimators and verifier-free training. GARL recovers RB-REINFORCE [$q=0$; Zhou et al., 2026] and the IWAE gradient [$q=1$; Burda et al., 2015]. Rainforth et al. [2018] showed IWAE’s inference-network gradient SNR shrinks as M grows, motivating doubly reparameterized variants [Roeder et al., 2017, Tucker et al., 2019]; our bias expansion $O(q/MP_\theta^q)$ exposes a related phenomenon along the J_Q continuum, with intermediate q balancing escape against estimator quality. Zhou et al. [2026] introduce VeriFree, the RB-REINFORCE estimator GARL extends; while Rao–Blackwellization reduces variance, Section 5 shows it does not address the cold-start escape bottleneck. Both GARL and PAFT are verifier-free across the J_Q continuum. Finally, Yue et al. [2025] observed that RLVR narrows the reasoning capability boundary during training; our framework attributes this to mode-seeking at $q=0$ (Corollary C.2), with PAFT (Section 4.2) an empirically more stable alternative to GARL during warm-start training (Section 5).

B Proofs for Section 2: Setup and Background

Proposition B.1 (RLVR connection). *Under the conditional model of Section 2 and exact-match reward $R(\hat{\mathbf{y}}, \mathbf{y}^*) = \mathbb{I}(\hat{\mathbf{y}} = \mathbf{y}^*)$, the expected reward equals $\mathbb{E}_{\mathcal{D}}[P_\theta]$; consequently $J_0(\theta) = 1 - \mathbb{E}_{\mathcal{D}}[P_\theta]$, and minimizing J_0 is equivalent to maximizing expected reward.*

Proof. For a fixed example $(\mathbf{x}^*, \mathbf{y}^*)$,

$$\begin{aligned} & \mathbb{E}_{\substack{\mathbf{z} \sim p_{\theta}(\cdot | \mathbf{x}^*), \\ \hat{\mathbf{y}} \sim p_{\theta}(\cdot | \mathbf{x}^*, \mathbf{z})}} [R(\hat{\mathbf{y}}, \mathbf{y}^*)] \\ &= \sum_{\substack{\mathbf{z} \in \mathcal{Z}, \\ \mathbf{y} \in \mathcal{Y}}} \left[p_{\theta}(\mathbf{z} | \mathbf{x}^*) \right. \\ & \quad \left. \cdot p_{\theta}(\mathbf{y} | \mathbf{x}^*, \mathbf{z}) \mathbb{I}(\mathbf{y} = \mathbf{y}^*) \right]. \end{aligned}$$

The indicator picks out the correct output, giving

$$\begin{aligned} \mathbb{E}_{\substack{\mathbf{z} \sim p_{\theta}(\cdot | \mathbf{x}^*), \\ \hat{\mathbf{y}} \sim p_{\theta}(\cdot | \mathbf{x}^*, \mathbf{z})}} [R(\hat{\mathbf{y}}, \mathbf{y}^*)] &= \sum_{\mathbf{z} \in \mathcal{Z}} p_{\theta}(\mathbf{z} | \mathbf{x}^*) p_{\theta}(\mathbf{y}^* | \mathbf{x}^*, \mathbf{z}) \\ &= P_{\theta}. \end{aligned}$$

Taking an expectation over training examples from \mathcal{D} , we have

$$\mathbb{E}_{\substack{(\mathbf{x}^*, \mathbf{y}^*) \sim \mathcal{D} \\ \mathbf{z} \sim p_{\theta}(\cdot | \mathbf{x}^*), \\ \hat{\mathbf{y}} \sim p_{\theta}(\cdot | \mathbf{x}^*, \mathbf{z})}} [R(\hat{\mathbf{y}}, \mathbf{y}^*)] = \mathbb{E}_{(\mathbf{x}^*, \mathbf{y}^*) \sim \mathcal{D}} [P_{\theta}].$$

□

C Proofs for Section 2: Loss Landscape

Proposition C.1 (Dispersion penalty). *For $q > 0$, $J_Q(\boldsymbol{\theta}, q) \geq -\log_q(\bar{P})$, where $\bar{P} \triangleq \mathbb{E}_{(\mathbf{x}^*, \mathbf{y}^*) \sim \mathcal{D}} [P_{\theta}]$ is the mean success probability across examples, with equality if and only if P_{θ} is constant across all examples in \mathcal{D} .*

Proof. For $q > 0$, the function $h_q(u) = -\log_q(u) = \frac{1-u^{1-q}}{1-q}$ is strictly convex on $(0, 1]$, since $h_q''(u) = qu^{-q-1} > 0$. Applying Jensen's inequality:

$$\begin{aligned} J_Q(\boldsymbol{\theta}, q) &= \mathbb{E}_{(\mathbf{x}^*, \mathbf{y}^*) \sim \mathcal{D}} [h_q(P_{\theta})] \\ &\geq h_q\left(\mathbb{E}_{(\mathbf{x}^*, \mathbf{y}^*) \sim \mathcal{D}} [P_{\theta}]\right) = -\log_q(\bar{P}), \end{aligned}$$

with equality iff P_{θ} is constant across all examples. □

Theorem 2.1. *[Minimizers of J_Q in the categorical model] For $q \in (0, 1]$, the unique minimizer of $J_Q(\boldsymbol{\theta}, q) = \sum_j \alpha_j (-\log_q \theta_j)$ over $\boldsymbol{\theta} \in \Delta_K$ is $\theta_j^*(q) = \frac{\alpha_j^{1/q}}{\sum_k \alpha_k^{1/q}}$. For $q = 0$, any vertex e_j with $j \in \arg\max_k \alpha_k$ is optimal.*

Proof. Case $q \in (0, 1]$. Since h_q is strictly convex for $q > 0$, the objective is strictly convex on the interior of Δ_K , and the minimizer is unique. Since all $\alpha_j > 0$, the minimizer lies in the interior (any boundary point has infinite loss for $q = 1$ and suboptimal loss for $q < 1$), so we can use Lagrange multipliers for the equality constraint $\sum_j \theta_j = 1$:

$$-\alpha_j \theta_j^{-q} - \lambda = 0 \quad \implies \quad \alpha_j \theta_j^{-q} = \mu \quad \text{for all } j,$$

where $\mu \triangleq -\lambda > 0$. Solving: $\theta_j = (\alpha_j / \mu)^{1/q}$. The constraint $\sum_j \theta_j = 1$ yields $\mu^{1/q} = \sum_k \alpha_k^{1/q}$, giving $\theta_j^*(q) = \alpha_j^{1/q} / \sum_k \alpha_k^{1/q}$ as in Theorem 2.1.

Case $q = 0$. The objective $J_Q(\boldsymbol{\theta}, 0) = 1 - \sum_j \alpha_j \theta_j$ is linear, minimized at any vertex e_j with $j \in \arg\max_k \alpha_k$. □

Corollary C.2 (Endpoint behavior and monotone sharpening). *Under the categorical model:*

1. **Density-estimation pole** ($q = 1$): $\theta_j^*(1) = \alpha_j$. The model exactly recovers the data distribution.
2. **Exploitation pole** ($q \rightarrow 0^+$): assuming a unique mode $j^* = \operatorname{argmax}_k \alpha_k$, $\theta_j^*(q) \rightarrow \mathbb{I}(j = j^*)$. The model concentrates all mass on the most frequent output.
3. **Monotone sharpening**: for $0 < q' < q \leq 1$ and $\alpha_j > \alpha_k$, $\theta_j^*(q')/\theta_k^*(q') > \theta_j^*(q)/\theta_k^*(q)$.

Proof. Part (1): $1/q = 1$. Part (2): $(\alpha_j/\alpha_{j^*})^{1/q} \rightarrow 0$ for $j \neq j^*$. Part (3): $\theta_j^*/\theta_k^* = (\alpha_j/\alpha_k)^{1/q}$, increasing in $1/q$. \square

Corollary C.3 (Propriety). *The Tsallis q -logarithmic scoring rule is strictly proper if and only if $q = 1$.*

Proof. By Theorem 2.1, the maximizer of $\mathbb{E}_{y \sim \alpha}[\log_q(\theta_y)]$ is $\theta_j^* \propto \alpha_j^{1/q}$, which equals α iff $q = 1$. For $q \in (0, 1)$ the true distribution α is not even a maximizer (the rule is not proper at all), let alone the unique one. \square

The robustness counterpart under label noise — both static (where the escort minimizer concentrates) and dynamic (how fast the model gets there) — appears in Section D.5.

D Proofs for Section 3: Commitment Dynamics under Gradient Flow

D.1 Warm-up: exact analysis on the sigmoid model

Before proving the general results, we work through the scalar sigmoid model $P(\theta) = \sigma(\theta) = (1 + e^{-\theta})^{-1}$ as a warm-up. This model admits exact closed-form escape times that validate the $\Theta(\cdot)$ bounds in Theorem 3.2.

Under gradient flow on $\ell_q(\theta) = -\log_q(\sigma(\theta))$, the parameter evolves as $\dot{\theta} = P(\theta)^{-q}P'(\theta)$. Since $P'(\theta) = P(\theta)(1 - P(\theta))$, the chain rule gives:

$$\dot{p} = [P'(\theta)]^2 P(\theta)^{-q} = p^{2-q}(1-p)^2.$$

This is a special case of the general dynamics (Equation (3)) with score norm $\|s(\theta)\|^2 = (1-p)^2$, which satisfies $\|s\|^2 \in [(1-\delta)^2, 1]$ on $p \in [p_0, \delta]$ — confirming the bounded score assumption.

The separable ODE gives the exact escape time:

$$T_q(p_0, \delta) = \int_{p_0}^{\delta} \frac{du}{u^{2-q}(1-u)^2}. \quad (10)$$

We evaluate this integral using a dominant/remainder decomposition. Write $(1-u)^{-2} = 1 + r(u)$ where $r(u) = \frac{2u-u^2}{(1-u)^2}$. On $u \in [0, \delta]$ with $\delta \leq 1/2$, we have $0 \leq r(u) \leq 8u$. Substituting and distributing:

$$T_q(p_0, \delta) = \underbrace{\int_{p_0}^{\delta} \frac{du}{u^{2-q}}}_{\text{dominant}} + \underbrace{\int_{p_0}^{\delta} \frac{r(u)}{u^{2-q}} du}_{\text{remainder}}.$$

Case $q \in (0, 1)$. The dominant integral evaluates to $\frac{p_0^{-(1-q)} - \delta^{-(1-q)}}{1-q} = \frac{p_0^{-(1-q)}}{1-q}(1 + o(1))$. The remainder satisfies $0 \leq \int r(u) u^{-(2-q)} du \leq 8 \int u^{q-1} du = \frac{8\delta^q}{q}$, a constant. So the remainder is negligible and $T_q = \frac{p_0^{-(1-q)}}{1-q}(1 + o(1))$.

Case $q = 0$. The dominant integral gives $\frac{1}{p_0}(1 + o(1))$. The remainder is $O(\log(1/p_0))$, still negligible compared to $1/p_0$. So $T_0 = \frac{1}{p_0}(1 + o(1))$.

Case $q = 1$. The dominant integral is $\log(1/p_0) + \log \delta$. The remainder satisfies $\int r(u) u^{-1} du \leq 8(\delta - p_0) = O(1)$. So $T_1 = \log(1/p_0)(1 + o(1))$.

Note that the sigmoid model yields exact $1 + o(1)$ asymptotics (not just $\Theta(\cdot)$) because $\|s\|^2 = (1-p)^2 \rightarrow 1$ as $p \rightarrow 0$, so the score norm converges to a known constant. This is stronger than the general theorem, which only assumes bounded score norms.

D.2 Proof of Theorem 3.1: Exploitation is provably slow

Theorem 3.1. [Exploitation is provably slow] Let $\theta \in \mathbb{R}^d$ parameterize any differentiable model. Consider gradient flow on $\ell_q(\theta) = -\log_q(P_\theta)$, starting from $p_0 = P_{\theta(0)} \in (0, 1/2)$ with fixed target $\delta \in (p_0, 1/2]$. Suppose $\|s(\theta(t))\| \leq C \in \mathbb{R}$. Then as $p_0 \rightarrow 0$:

$$T_q(p_0, \delta) = \Omega\left(\frac{p_0^{-(1-q)}}{1-q}\right) \text{ for } q \in [0, 1),$$

$$T_1(p_0, \delta) = \Omega\left(\log \frac{1}{p_0}\right).$$

Proof. From Equation (3), $\dot{p} = p^{2-q}\|s(\theta)\|^2 \leq C^2 p^{2-q}$. By the ODE comparison principle (since $u \mapsto u^{2-q}$ is nondecreasing on $(0, 1]$), $p(t) \leq p^*(t)$ where p^* solves $\dot{p}^* = C^2(p^*)^{2-q}$ with $p^*(0) = p_0$. So p reaches δ no sooner than p^* :

$$T_q \geq \frac{1}{C^2} \int_{p_0}^{\delta} \frac{du}{u^{2-q}}.$$

For $q \in [0, 1)$, the integral evaluates to $\frac{p_0^{-(1-q)} - \delta^{-(1-q)}}{1-q} = \frac{p_0^{-(1-q)}}{1-q}(1 + o(1))$, giving $T_q = \Omega(p_0^{-(1-q)}/(1-q))$.

For $q = 1$, the integral is $\log(\delta/p_0) = \log(1/p_0)(1 + o(1))$, giving $T_1 = \Omega(\log(1/p_0))$. \square

D.3 Proof of Theorem 3.2: Tight cold-start escape rates

Theorem 3.2. [Tight cold-start escape rates] Under the same setup as Theorem 3.1, suppose additionally that $\|s(\theta(t))\| \geq c > 0$ throughout the trajectory. Then as $p_0 \rightarrow 0$,

$$T_q(p_0, \delta) = \Theta\left(\frac{p_0^{-(1-q)}}{1-q}\right) \text{ for } q \in [0, 1), \quad T_1(p_0, \delta) = \Theta\left(\log \frac{1}{p_0}\right),$$

and consequently $T_q(p_0, \delta)/T_{q'}(p_0, \delta) \rightarrow \infty$ for any $q < q' \leq 1$.

Proof. The lower bound on time (Ω) follows from Theorem 3.1. For the upper bound, the additional assumption $\|s\| \geq c > 0$ gives $\dot{p} \geq c^2 p^{2-q}$; by the ODE comparison principle, $p(t) \geq p_*(t)$ where p_* solves $\dot{p}_* = c^2(p_*)^{2-q}$, so p reaches δ no later than p_* :

$$T_q \leq \frac{1}{c^2} \int_{p_0}^{\delta} \frac{du}{u^{2-q}}.$$

This integral evaluates to $\frac{p_0^{-(1-q)}}{1-q}(1 + o(1))$ for $q \in [0, 1)$ and $\log(1/p_0)(1 + o(1))$ for $q = 1$. Combined with the lower bound, $T_q = \Theta(p_0^{-(1-q)}/(1-q))$ for $q < 1$ and $T_1 = \Theta(\log(1/p_0))$.

Speedup ratio. For $q < q' < 1$: $T_q/T_{q'} = \Theta(p_0^{-(q'-q)}) \rightarrow \infty$. For $q < 1$ and $q' = 1$: $T_q/T_1 = \Theta(p_0^{-(1-q)}/\log(1/p_0)) \rightarrow \infty$. \square

D.4 Near-optimality convergence (supplementary result)

Proposition D.1 (Near-optimality convergence is q -independent). Suppose that near optimality, $\|s(\theta)\|^2$ depends on θ only through P_θ (i.e., $\|s(\theta)\|^2 = h(P_\theta)$ for some function h). Then for $\epsilon_0 \ll 1$ and $\epsilon_1 < \epsilon_0$, the time to improve from $P_\theta = 1 - \epsilon_0$ to $P_\theta = 1 - \epsilon_1$ satisfies

$$T_q(1 - \epsilon_0, 1 - \epsilon_1) = T_{q'}(1 - \epsilon_0, 1 - \epsilon_1)(1 + O(\epsilon_0))$$

for all $q, q' \in [0, 1]$. That is, the convergence time is the same for all members of the J_Q family up to a correction that vanishes as $\epsilon_0 \rightarrow 0$.

Proof. Write $\epsilon = 1 - p$ with $\epsilon \ll 1$. From Equation (3), $\dot{\epsilon} = -(1 - \epsilon)^{2-q} \|s(\boldsymbol{\theta})\|^2 < 0$. Since ϵ decreases over time, the convergence time from ϵ_0 to ϵ_1 is:

$$T_q = \int_{\epsilon_1}^{\epsilon_0} \frac{d\epsilon}{(1 - \epsilon)^{2-q} \|s(\boldsymbol{\theta})\|^2}.$$

For any $q, q' \in [0, 1]$, the integrands of T_q and $T_{q'}$ differ by the factor $(1 - \epsilon)^{q-q'}$. We bound this factor on $\epsilon \in [\epsilon_1, \epsilon_0]$ with $\epsilon_0 \ll 1$. Using the Taylor expansion $\log(1 - \epsilon) = -\epsilon - \epsilon^2/2 - \dots$:

$$\begin{aligned} \log(1 - \epsilon)^{q-q'} &= (q - q') \log(1 - \epsilon) \\ &= (q - q') \left(-\epsilon - \frac{\epsilon^2}{2} - \dots \right). \end{aligned}$$

Since $|q - q'| \leq 1$:

$$|\log(1 - \epsilon)^{q-q'}| \leq \epsilon + \frac{\epsilon^2}{2} + \dots = O(\epsilon).$$

Exponentiating and using $e^x = 1 + x + O(x^2) = 1 + O(\epsilon)$ for $x = O(\epsilon)$, we get $(1 - \epsilon)^{q-q'} = 1 + O(\epsilon)$. Since $\epsilon \leq \epsilon_0$ on $[\epsilon_1, \epsilon_0]$, the integrands of T_q and $T_{q'}$ differ by a multiplicative $1 + O(\epsilon_0)$ factor, giving $T_q/T_{q'} = 1 + O(\epsilon_0)$. \square

D.5 Noise-fitting rate under symmetric label noise

The cold-start escape rates (Theorems 3.1 and 3.2) measure how fast the model commits to correct supervision under the J_Q amplification $P_{\boldsymbol{\theta}}^{-q}$. The symmetric question is how fast the model commits to *incorrect* supervision: the same amplification drives both, giving the following dynamical formulation of robustness under label noise.

Noise-contamination setup. We work with a two-label categorical model, chosen to expose the mechanism in the simplest possible setting. For a single input \mathbf{x}^* , the model predicts one of two labels $\{c, k\}$ with probabilities $p_{\boldsymbol{\theta}}(c | \mathbf{x}^*) = p$ and $p_{\boldsymbol{\theta}}(k | \mathbf{x}^*) = 1 - p$. We instantiate the parameterization with the sigmoid $p = \sigma(\theta)$ used in Section D.1, under which $s \triangleq \nabla_{\theta} \log p = \tilde{p}$ and $\|s\|^2 = \tilde{p}^2$. The target label is *corrupted*: with probability $1 - \epsilon$ it equals the clean value c , and with probability $\epsilon \in (0, 1/2)$ it flips to the noise value k , giving $\tilde{\alpha} = (1 - \epsilon, \epsilon)$. The restriction to two labels is cosmetic: in the N -label categorical model with symmetric noise $\tilde{\alpha} = (1 - \epsilon)\alpha + \epsilon \cdot \text{Unif}$, conditioning on the two-subset $\{j^*, k\}$ containing the clean mode j^* and any fixed wrong label k reduces to this binary setting.

Let $p(t) = p_{\boldsymbol{\theta}}(c | \mathbf{x}^*)$ denote the clean-mode probability under gradient flow on $J_Q(\boldsymbol{\theta}) = \mathbb{E}_{y \sim \tilde{\alpha}} [\ell_q(p_{\boldsymbol{\theta}}(y | \mathbf{x}^*))]$, and let $\tilde{p}(t) = 1 - p(t)$ denote the noise contamination. The cold-start analysis (Theorem 3.2) assumed a non-vanishing score $\|s\| \geq c_* > 0$; the analogous lower bound fails near $p = 1$, where the sigmoid score vanishes linearly in \tilde{p} , so we substitute the actual scaling $\|s\|^2 = \tilde{p}^2$ rather than treating $\|s\|$ as a constant.

The escort asymptote. Differentiating $J(p) = (1 - \epsilon)\ell_q(p) + \epsilon\ell_q(1 - p)$ gives $J'(p) = -(1 - \epsilon)p^{-q} + \epsilon\tilde{p}^{-q}$. Gradient flow on the sigmoid yields

$$\dot{\tilde{p}} = -\dot{p} = [\epsilon\tilde{p}^{-q} - (1 - \epsilon)(1 - \tilde{p})^{-q}] p^2 \tilde{p}^2. \quad (11)$$

For $q > 0$, the dynamics have a unique stable equilibrium at

$$\tilde{p}_*(q) = (\epsilon/(1 - \epsilon))^{1/q} (1 + o(1)) \quad \text{as } \epsilon \rightarrow 0, \quad (12)$$

obtained by solving $J'(p) = 0$ ($\|s\|^2$ cancels at equilibrium, so $\tilde{p}_*(q)$ does not depend on the parameterization). This equilibrium coincides with the static escort minimizer from Theorem 2.1 applied to $\tilde{\alpha}$: at $q = 1$, $\tilde{p}_*(1) = \epsilon$ (the model fits observed noise exactly); as $q \rightarrow 0$, $\tilde{p}_*(q) \rightarrow 0$ (the model concentrates on the clean mode, paralleling Corollary C.2). The escort is both where J_Q is minimized (static) and where gradient flow converges (dynamic).

The noise-to-clean ratio $\epsilon \tilde{p}^{-q} / [(1 - \epsilon)(1 - \tilde{p})^{-q}]$ is monotone decreasing in \tilde{p} on $(0, 1)$: it diverges as $\tilde{p} \rightarrow 0$ (noise term dominates near the clean mode), equals 1 at $\tilde{p} = \tilde{p}_*(q)$ (equilibrium), and vanishes as $\tilde{p} \rightarrow 1$. So for $\tilde{p} \ll \tilde{p}_*(q)$ — the regime of small noise contamination — the noise term in Equation (11) dominates by an arbitrarily large factor. This drives the asymptotic scaling.

Proposition D.2 (Noise-fitting rate). *Fix $q \in (0, 1]$. Under the setup above, starting from $\tilde{p}(0) = \tilde{p}_0$ with $\tilde{p}_0 \ll \tilde{p}_*(q)$, the time $T_q^{\text{noise}}(\tilde{p}_0)$ to reach a fixed target η (with $\tilde{p}_0 \ll \eta \leq \tilde{p}_*(q)$, η independent of \tilde{p}_0) satisfies, as $\tilde{p}_0 \rightarrow 0$:*

$$T_q^{\text{noise}}(\tilde{p}_0) = \Theta\left(\frac{\tilde{p}_0^{-(1-q)}}{(1-q)\epsilon}\right) \text{ for } q \in (0, 1), \quad T_1^{\text{noise}}(\tilde{p}_0) = \Theta\left(\frac{\log(1/\tilde{p}_0)}{\epsilon}\right). \quad (13)$$

The speedup ratio for $0 < q < q' \leq 1$ diverges: $T_q^{\text{noise}}(\tilde{p}_0)/T_{q'}^{\text{noise}}(\tilde{p}_0) = \Theta(\tilde{p}_0^{-(q'-q)}) \rightarrow \infty$ as $\tilde{p}_0 \rightarrow 0$. At $q = 0$, adopting the convention $\tilde{p}^0 \equiv 1$, the dynamics Equation (11) reduce to $\dot{\tilde{p}} = -(1 - 2\epsilon)p^2 \tilde{p}^2 < 0$ everywhere (for $\epsilon < 1/2$), so any positive \tilde{p}_0 decays monotonically toward 0: $T_0^{\text{noise}}(\tilde{p}_0) = \infty$ for any target $\eta > \tilde{p}_0$.

Proof. By the noise-to-clean monotonicity established above, for any $K > 1$ there exists $\tilde{p}_K(q) = K^{-1/q} \tilde{p}_*(q)(1 + o(1))$ such that for $\tilde{p} \leq \tilde{p}_K$, the noise term in Equation (11) exceeds K times the clean term. Combined with $p = 1 - \tilde{p} \rightarrow 1$ as $\tilde{p} \rightarrow 0$ and $\|s\|^2 = \tilde{p}^2$:

$$\dot{\tilde{p}} \in \left[(1 - \frac{1}{K})\epsilon \tilde{p}^{2-q} (1 + o(1)), \epsilon \tilde{p}^{2-q}\right].$$

Fix any $K > 1$ (e.g., $K = 2$). Separating variables, $\tilde{p}^{q-2} d\tilde{p} = \Theta(\epsilon) dt$. For $q \in (0, 1)$, integrating from \tilde{p}_0 to η with $\tilde{p}_0 \ll \eta \leq \tilde{p}_K(q)$ gives

$$\frac{\tilde{p}_0^{-(1-q)} - \eta^{-(1-q)}}{1-q} = \Theta(\epsilon T),$$

so $T_q^{\text{noise}}(\tilde{p}_0) = \Theta(\tilde{p}_0^{-(1-q)} / ((1-q)\epsilon))$ as $\tilde{p}_0 \rightarrow 0$. (The integral from exactly $\tilde{p}_0 = 0$ diverges for $q \leq 1$, so a positive starting contamination is required.) For $q = 1$, $\dot{\tilde{p}} = \Theta(\epsilon \tilde{p})$ gives $\tilde{p}(t) = \tilde{p}_0 \exp(\Theta(\epsilon t))$, so $T_1^{\text{noise}}(\tilde{p}_0) = \Theta(\log(\eta/\tilde{p}_0)/\epsilon) = \Theta(\log(1/\tilde{p}_0)/\epsilon)$. The speedup ratio $T_q/T_{q'} = \Theta(\tilde{p}_0^{-(q'-q)})$ diverges for $q < q' \leq 1$ as $\tilde{p}_0 \rightarrow 0$. \square

Structural parallel with cold-start escape. Theorem 3.2 gives $T_q^{\text{escape}}(p_0) = \Theta(p_0^{-(1-q)} / (1 - q))$ for $q < 1$ and $\Theta(\log(1/p_0))$ at $q=1$, with speedup ratio $\Theta(p_0^{-(q'-q)})$. Proposition D.2 gives $T_q^{\text{noise}}(\tilde{p}_0) = \Theta(\tilde{p}_0^{-(1-q)} / ((1-q)\epsilon))$ and $\Theta(\log(1/\tilde{p}_0)/\epsilon)$, with speedup ratio $\Theta(\tilde{p}_0^{-(q'-q)})$ — the *exact dual*: same exponent in the small starting probability (p_0 for cold-start escape from clean, \tilde{p}_0 for noise-fitting escape from corruption), with the noise rate ϵ as the only additional rate factor. The same P_θ^{-q} amplification accelerates commitment to clean and corrupted supervision by the same multiplicative factor. Static mode-seeking (Corollary C.2) is recovered as the $t \rightarrow \infty$ limit of Equation (11): $\tilde{p}(t) \rightarrow \tilde{p}_*(q) \rightarrow 0$ as $q \rightarrow 0$.

E Proofs and Pseudocode for Section 4: Monte Carlo Estimators

Theorem 4.1. *[Consistency and bias expansion] Fix a supervised example $(\mathbf{x}^*, \mathbf{y}^*)$ and assume:*

1. $P_\theta > 0$;
2. $\mathbb{E}[\|g_m\|^2] < \infty$;
3. $w_m \geq \epsilon$ a.s. for some $\epsilon > 0$.

Then for any fixed $q \in [0, 1]$, the estimator is consistent: $\hat{\nabla}_\theta \ell_q \xrightarrow{\text{a.s.}} \nabla_\theta \ell_q$ as $M \rightarrow \infty$. Moreover, the leading-order bias is

$$\mathbb{E}\left[\hat{\nabla}_\theta \ell_q\right] - \nabla_\theta \ell_q = \frac{q}{MP_\theta^{q+1}} \left[\frac{q+1}{2} \nabla_\theta \ell_1 \mathbf{Var}(w_m) - \mathbf{Cov}(g_m, w_m)\right] + O(M^{-2}) \quad \text{as } M \rightarrow \infty. \quad (7)$$

Under additionally bounded marginal and per-trajectory scores ($\|\nabla_\theta \log P_\theta\| \leq C$, $\|\nabla_\theta \log p_\theta(\mathbf{z}, \mathbf{y}^ | \mathbf{x}^*)\| \leq C'$), the bracketed term is $O(P_\theta)$, so the bias simplifies to $O(q/MP_\theta^q)$.*

Proof. We write

$$\mu_w \triangleq \mathbb{E}[w_m] = P\boldsymbol{\theta}, \quad \mu_g \triangleq \mathbb{E}[g_m] = \nabla_{\boldsymbol{\theta}} \ell_0(\boldsymbol{\theta}; \mathbf{x}^*, \mathbf{y}^*).$$

Define the smooth map

$$f(a, b) \triangleq b a^{-q},$$

for $a > 0$. Then

$$\hat{\nabla}_{\boldsymbol{\theta}} \ell_q(q, \boldsymbol{\theta}; \mathbf{x}^*, \mathbf{y}^*, M) = f(\bar{w}_M, \bar{g}_M),$$

while the target gradient is

$$\nabla_{\boldsymbol{\theta}} \ell_q(\boldsymbol{\theta}, q; \mathbf{x}^*, \mathbf{y}^*) = f(\mu_w, \mu_g) = \mu_g \mu_w^{-q}.$$

Almost sure convergence follows from the Strong Law of Large Numbers, since $\bar{w}_M \rightarrow \mu_w$ and $\bar{g}_M \rightarrow \mu_g$ almost surely, and f is continuous at (μ_w, μ_g) because $\mu_w = P\boldsymbol{\theta} > 0$.

For the bias expansion, we exploit the linearity of f in its second argument: $f(a, b) = b a^{-q}$, so

$$\begin{aligned} f(\bar{w}_M, \bar{g}_M) &= \bar{g}_M \cdot h(\bar{w}_M) \\ &= \underbrace{\mu_g h(\bar{w}_M)}_{\text{first piece}} + \underbrace{(\bar{g}_M - \mu_g) h(\bar{w}_M)}_{\text{second piece}}, \end{aligned}$$

where $h(a) \triangleq a^{-q}$ is a scalar function whose derivatives $h^{(k)}(a) = (-q)(-q-1)\cdots(-q-k+1) a^{-(q+k)}$ depend only on a .

First piece. Expand $h(\bar{w}_M)$ to *third* order around μ_w , with $h'(a) = -q a^{-q-1}$, $h''(a) = q(q+1) a^{-q-2}$, $h'''(a) = -q(q+1)(q+2) a^{-q-3}$:

$$\begin{aligned} h(\bar{w}_M) &= \underbrace{h(\mu_w)}_{\mathbb{E}[\cdot] = \mu_w^{-q}} + \underbrace{h'(\mu_w)(\bar{w}_M - \mu_w)}_{\mathbb{E}[\cdot] = 0} + \underbrace{\frac{1}{2} h''(\mu_w)(\bar{w}_M - \mu_w)^2}_{\mathbb{E}[\cdot] = \frac{q(q+1)}{2M} \mu_w^{-q-2} \mathbf{Var}(w_m)} \\ &\quad + \underbrace{\frac{1}{6} h'''(\mu_w)(\bar{w}_M - \mu_w)^3}_{\mathbb{E}[\cdot] = O(M^{-2}) \text{ via } \kappa_3/M^2} + \underbrace{R_M^{(1)}}_{\text{4th-order}}. \end{aligned}$$

Therefore:

$$\begin{aligned} \mu_g \mathbb{E}[h(\bar{w}_M)] &= \mu_g \mu_w^{-q} + \frac{q(q+1)}{2M} \mu_g \mu_w^{-q-2} \mathbf{Var}(w_m) \\ &\quad + O(M^{-2}) + \mu_g \mathbb{E}[R_M^{(1)}]. \end{aligned}$$

Second piece. The factor $(\bar{g}_M - \mu_g) = O_p(M^{-1/2})$, so a *second*-order expansion of $h(\bar{w}_M)$ suffices. Multiplying $(\bar{g}_M - \mu_g)$ by each term of the expansion and taking expectations:

$$\begin{aligned} &\mathbb{E}[(\bar{g}_M - \mu_g) h(\bar{w}_M)] \\ &= \underbrace{h(\mu_w) \mathbb{E}[\bar{g}_M - \mu_g]}_{=0} + \underbrace{h'(\mu_w) \mathbb{E}[(\bar{g}_M - \mu_g)(\bar{w}_M - \mu_w)]}_{=-\frac{q}{M} \mu_w^{-q-1} \mathbf{Cov}(g_m, w_m)} \\ &\quad + \underbrace{\frac{1}{2} h''(\mu_w) \mathbb{E}[(\bar{g}_M - \mu_g)(\bar{w}_M - \mu_w)^2]}_{=O(M^{-2}) \text{ via i.i.d. expansion}} + \underbrace{\mathbb{E}[R_M^{(2)}]}_{\text{3rd-order remainder}}. \end{aligned}$$

For the cross moment, expand $\mathbb{E}[(\bar{g}_M - \mu_g)(\bar{w}_M - \mu_w)^2] = M^{-3} \sum_{i,j,k} \mathbb{E}[(g_i - \mu_g)(w_j - \mu_w)(w_k - \mu_w)]$. By independence, the only nonzero index pattern is $i = j = k$ (all others vanish because $\mathbb{E}[g_i - \mu_g] = 0$ or $\mathbb{E}[w_j - \mu_w] = 0$). The M surviving terms give $\mathbb{E}[(g_m - \mu_g)(w_m - \mu_w)^2]/M^2 = O(M^{-2})$, since $|(w_m - \mu_w)^2| \leq 1$ and $\mathbb{E}[|g_m|] < \infty$ (Assumption 2). The remainder has the form $R_M^{(2)} = (\bar{g}_M - \mu_g) \cdot O(|\bar{w}_M - \mu_w|^3)$.

Combining. Adding the two pieces and substituting $\mu_w = P_\theta$, $\mu_g = \nabla_\theta \ell_0$, $\nabla_\theta \ell_1 = \nabla_\theta \ell_0 / P_\theta$:

$$\begin{aligned} \mathbb{E}\left[\hat{\nabla}_\theta \ell_q(q, \theta; \mathbf{x}^*, \mathbf{y}^*, M)\right] &= \nabla_\theta \ell_q(\theta, q; \mathbf{x}^*, \mathbf{y}^*) \\ &+ \frac{q}{MP_\theta^{q+1}} \cdot \left[\frac{q+1}{2} \nabla_\theta \ell_1(\theta; \mathbf{x}^*, \mathbf{y}^*) \mathbf{Var}(w_m) - \mathbf{Cov}(g_m, w_m) \right] \\ &+ \mathbb{E}[R_M], \end{aligned} \tag{14}$$

where $R_M = \mu_g R_M^{(1)} + R_M^{(2)}$.

Remainder bound. Write $\mathbb{E}[R_M] = \mathbb{E}[R_M \cdot \mathbf{1}_A] + \mathbb{E}[R_M \cdot \mathbf{1}_{A^c}]$ where $A = \{\bar{w}_M \geq P_\theta/2\}$.

On A. The derivatives of h are bounded on $\{a \geq P_\theta/2\}$: $|h^{(k)}(a)| \leq C_k$.

For $R_M^{(1)}$ (the *fourth-order* scalar remainder), the integral form gives $|R_M^{(1)}| \leq C_4 |\bar{w}_M - \mu_w|^4$ on A . Since $w_m \in [0, 1]$, $\mathbb{E}[|\bar{w}_M - \mu_w|^4] = O(M^{-2})$, so $\mathbb{E}[|R_M^{(1)}| \cdot \mathbf{1}_A] = O(M^{-2})$.

For $R_M^{(2)} = (\bar{g}_M - \mu_g) \cdot O(|\bar{w}_M - \mu_w|^3)$ on A (the *third-order* remainder from the second piece, a vector quantity), Cauchy–Schwarz gives $\mathbb{E}[|R_M^{(2)}| \cdot \mathbf{1}_A] \leq C_3 \sqrt{\mathbb{E}[|\bar{g}_M - \mu_g|^2]} \sqrt{\mathbb{E}[|\bar{w}_M - \mu_w|^6]} = O(M^{-1/2}) O(M^{-3/2}) = O(M^{-2})$, using Assumption 2 and the boundedness of w_m .

On A^c. Assumption 3 gives $\bar{w}_M \geq \epsilon > 0$, so $|h(\bar{w}_M)| \leq \epsilon^{-q}$ everywhere and $\|f(\bar{w}_M, \bar{g}_M)\| \leq \epsilon^{-q} \|\bar{g}_M\|$. Therefore $\|R_M\| \leq \|f(\bar{w}_M, \bar{g}_M)\| + \|T_M\| \leq C \epsilon^{-q} (1 + \|\bar{g}_M\|)$, where T_M collects the (bounded) Taylor terms. Again by Cauchy–Schwarz,

$$\mathbb{E}[|R_M| \cdot \mathbf{1}_{A^c}] \leq C \epsilon^{-q} \sqrt{\mathbb{E}[(1 + \|\bar{g}_M\|)^2]} \sqrt{P(A^c)}.$$

The first factor is $O(1)$ by Assumption 2. For the second, since $w_m \in [0, 1]$ are i.i.d. with mean P_θ , Hoeffding’s inequality with $t = P_\theta/2$ gives $P(A^c) = P(\bar{w}_M - P_\theta \leq -P_\theta/2) \leq \exp(-MP_\theta^2/2)$. Thus $\mathbb{E}[|R_M| \cdot \mathbf{1}_{A^c}]$ decays faster than any polynomial in M .

Combining: $\mathbb{E}[R_M] = O(M^{-2})$, so the leading-order bias is the explicit formula above.

Bound on the bracketed coefficient. In Equation (14), the prefactor $q/(MP_\theta^{q+1})$ has $P_\theta^{-(q+1)}$ scaling, but the bracket $[(q+1)/2 \nabla_\theta \ell_1 \mathbf{Var}(w_m) - \mathbf{Cov}(g_m, w_m)]$ scales as $O(P_\theta)$, so one factor of P_θ cancels. Specifically:

- $\mathbf{Var}(w_m) \leq \mathbb{E}[w_m^2] \leq \mathbb{E}[w_m] = P_\theta$ since $w_m \in [0, 1]$.
- $\nabla_\theta \ell_1 = -\nabla_\theta \log P_\theta = -s$ is bounded under the bounded-score assumption used in Theorem 3.1.
- Under bounded per-trajectory score $\|\nabla_\theta \log p_\theta(\mathbf{z}, \mathbf{y}^* | \mathbf{x}^*)\| \leq C'$ (which follows from bounded weights and Lipschitz activations), $\|g_m\| \leq C' w_m$, and Cauchy–Schwarz gives $\|\mathbf{Cov}(g_m, w_m)\| \leq \sqrt{\mathbf{Var}(g_m) \mathbf{Var}(w_m)} \leq \sqrt{C'^2 P_\theta \cdot P_\theta} = O(P_\theta)$.

Hence the bracket is bounded by $(q+1)/2 O(P_\theta) + O(P_\theta) = O(P_\theta)$ (the $(q+1)/2$ multiplier is bounded by 1 for $q \in [0, 1]$ and absorbs into the constant), and the leading-order bias is $q/(MP_\theta^{q+1}) \cdot O(P_\theta) = O(q/(MP_\theta^q))$, yielding Equation (7). The bias scales with the same P_θ^{-q} exponent as the cold-start amplification factor. \square

E.1 RLOO control variate derivation

We derive the RLOO estimator (17) from the plug-in estimator (6). Using the chain rule, g_m from (4) decomposes into a score-function term and a pathwise term:

$$g_m = -w_m \nabla_\theta \log p_\theta(\mathbf{z}^{(m)} | \mathbf{x}^*) - \nabla_\theta w_m. \tag{15}$$

Substituting into the plug-in estimator isolates the score-function component:

$$\hat{\nabla}_\theta^{\text{plug-in}} \ell_q = \frac{1}{M} \sum_{m=1}^M \left[\frac{-w_m}{(\bar{w}_M)^q} \nabla_\theta \log p_\theta(\mathbf{z}^{(m)} | \mathbf{x}^*) - \frac{\nabla_\theta w_m}{(\bar{w}_M)^q} \right]. \tag{16}$$

Since $\mathbb{E}[\nabla_{\theta} \log p_{\theta}(\mathbf{z}^{(m)} | \mathbf{x}^*)] = 0$, we can subtract any baseline from the score-function coefficient $-w_m/(\bar{w}_M)^q$ without changing the expected value, provided the baseline does not depend on $\mathbf{z}^{(m)}$.

We use a leave-one-out approximation. Let $\bar{w}_{-m} = \frac{1}{M-1} \sum_{j \neq m} w_j$. Replacing w_m with \bar{w}_{-m} in the coefficient, the batch mean collapses to \bar{w}_{-m} , giving a surrogate coefficient of $-(\bar{w}_{-m})^{1-q}$. Subtracting this baseline yields the RLOO estimator

$$\hat{\nabla}_{\theta}^{\text{RLOO}} \ell_q = \frac{1}{M} \sum_{m=1}^M \left[- \underbrace{\left(\frac{w_m}{(\bar{w}_M)^q} - (\bar{w}_{-m})^{1-q} \right)}_{\text{centered weight}} \cdot \nabla_{\theta} \log p_{\theta}(\mathbf{z}^{(m)} | \mathbf{x}^*) - \frac{\nabla_{\theta} w_m}{(\bar{w}_M)^q} \right]. \quad (17)$$

Endpoint recovery. At $q = 0$, the centered weight evaluates to $w_m - \bar{w}_{-m}$, and the score-function term becomes $-(w_m - \bar{w}_{-m}) \nabla_{\theta} \log p_{\theta}(\mathbf{z}^{(m)} | \mathbf{x}^*)$, exactly recovering the REINFORCE leave-one-out (RLOO) estimator standard in RLVR. At $q = 1$, the centered weight is $w_m/\bar{w}_M - 1$; since $\sum_{m=1}^M (w_m/\bar{w}_M - 1) = 0$, this acts as a self-normalizing baseline that strictly centers the importance weights across the batch.

Proposition E.1 (RLOO bias preservation). *Under the assumptions of Theorem 4.1, the RLOO estimator (17) satisfies the same bias expansion as the plug-in estimator (6).*

Proof. The RLOO estimator (17) differs from the plug-in estimator (16) by subtracting $(\bar{w}_{-m})^{1-q}$ from the score-function coefficient $w_m/(\bar{w}_M)^q$ for each sample m . Denoting $s_m = \nabla_{\theta} \log p_{\theta}(\mathbf{z}^{(m)} | \mathbf{x}^*)$, the difference in expectations is

$$\Delta = \frac{1}{M} \sum_{m=1}^M \mathbb{E}[(\bar{w}_{-m})^{1-q} s_m].$$

Since $\bar{w}_{-m} = \frac{1}{M-1} \sum_{j \neq m} w_j$ is a function of $\{\mathbf{z}^{(j)}\}_{j \neq m}$ only, and $s_m = \nabla_{\theta} \log p_{\theta}(\mathbf{z}^{(m)} | \mathbf{x}^*)$ is a function of $\mathbf{z}^{(m)}$ only, the independence of the i.i.d. samples gives

$$\mathbb{E}[(\bar{w}_{-m})^{1-q} s_m] = \mathbb{E}[(\bar{w}_{-m})^{1-q}] \cdot \underbrace{\mathbb{E}[s_m]}_{=0} = 0,$$

where $\mathbb{E}[s_m] = \mathbb{E}_{\mathbf{z} \sim p_{\theta}}[\nabla_{\theta} \log p_{\theta}(\mathbf{z} | \mathbf{x}^*)] = 0$ is the standard score-function identity. Therefore $\Delta = 0$ and the two estimators have identical expectations for every M . \square

E.2 Endpoint recovery

Proposition E.2 (Endpoint recovery for GARL and PAFT). *Fix a supervised example $(\mathbf{x}^*, \mathbf{y}^*)$ with $P_{\theta} > 0$.*

1. **GARL** at $q = 0$ recovers Rao-Blackwellized REINFORCE [Williams, 1992, Zhou et al., 2026]:

$$\hat{\nabla}_{\theta} \ell_q|_{q=0} = \bar{g}_M = \frac{1}{M} \sum_{m=1}^M (-w_m \nabla_{\theta} \log p_{\theta}(\mathbf{z}^{(m)}, \mathbf{y}^* | \mathbf{x}^*)),$$

which is unbiased for $\nabla_{\theta} \ell_0$ by Equation (5). Each g_m marginalizes out the output \mathbf{y} given $\mathbf{z}^{(m)}$ analytically via $w_m = p_{\theta}(\mathbf{y}^* | \mathbf{x}^*, \mathbf{z}^{(m)})$, rather than relying on a sampled output and binary reward.

2. **GARL** at $q = 1$ recovers the IWAE gradient estimator [Burda et al., 2015], a self-normalized importance sampling (SNIS) estimator for $\nabla_{\theta} \log P_{\theta}$:

$$\hat{\nabla}_{\theta} \ell_q|_{q=1} = \frac{\bar{g}_M}{\bar{w}_M} = \frac{\sum_m w_m (-\nabla_{\theta} \log p_{\theta}(\mathbf{z}^{(m)}, \mathbf{y}^* | \mathbf{x}^*))}{\sum_m w_m}.$$

3. **PAFT** at $q = 0$ reduces to posterior-resampled SFT scaled by P_{θ} :

$$\hat{\nabla}_{\text{PAFT}}|_{q=0} = -\bar{w}_M \cdot \frac{1}{K} \sum_{k=1}^K \nabla_{\theta} \log p_{\theta}(\mathbf{z}^{(r_k)}, \mathbf{y}^* | \mathbf{x}^*).$$

The factor $\bar{w}_M \approx P_\theta$ downweights hard instances so aggressively that this endpoint is overly conservative in practice. Unlike the other three endpoints, it does not correspond to a standard method.

4. **PAFT at $q = 1$ recovers the EM gradient update with E-step posterior samples [Dempster et al., 1977] / TRICE [Phan et al., 2023]:**

$$\hat{\nabla}_{\text{PAFT}}|_{q=1} = -\frac{1}{K} \sum_{k=1}^K \nabla_{\theta} \log p_{\theta}(\mathbf{z}^{(r_k)}, \mathbf{y}^* | \mathbf{x}^*).$$

The attenuation vanishes: $(\bar{w}_M)^{1-1} = 1$, so all instances contribute equally, and the gradient is uniform SFT on approximate posterior samples.

Proof. Each case follows by substituting $q = 0$ or $q = 1$ into the GARL estimator (6) or PAFT estimator (9) and simplifying $(\bar{w}_M)^0 = 1$. \square

E.3 PAFT bias and variance

Proposition E.3 (PAFT has the same bias as GARL). *Under the assumptions of Theorem 4.1, $\mathbb{E}[\hat{\nabla}_{\text{PAFT}}] = \mathbb{E}[\hat{\nabla}_{\text{GARL}}]$ for all M . In particular, the PAFT estimator inherits the same leading bias expansion as in Equation (7), simplifying to $O(q/M P_\theta^q)$ under bounded marginal and per-trajectory scores.*

Proof. Conditional on the prior samples pool = $\{(\mathbf{z}^{(m)}, w_m)\}_{m=1}^M$, the factor $(\bar{w}_M)^{1-q}$ is deterministic. The importance-resampled average satisfies

$$\mathbb{E} \left[\frac{1}{K} \sum_{k=1}^K f(\mathbf{z}^{(r_k)}) \mid \text{pool} \right] = \sum_{m=1}^M \frac{w_m}{\sum_j w_j} f(\mathbf{z}^{(m)}) = \hat{\mu}_{\text{SNIS}},$$

where $f(\mathbf{z}) = \nabla_{\theta} \log p_{\theta}(\mathbf{z}, \mathbf{y}^* | \mathbf{x}^*)$. Therefore

$$\begin{aligned} \mathbb{E}[\hat{\nabla}_{\text{PAFT}} | \text{pool}] &= -(\bar{w}_M)^{1-q} \cdot \hat{\mu}_{\text{SNIS}} \\ &= -(\bar{w}_M)^{1-q} \cdot \frac{\sum_m w_m f_m}{M \bar{w}_M} \\ &= \frac{1}{(\bar{w}_M)^q} \cdot \frac{1}{M} \sum_m (-w_m f_m) \\ &= \frac{\bar{g}_M}{(\bar{w}_M)^q} = \hat{\nabla}_{\text{GARL}}. \end{aligned}$$

Taking outer expectations by the tower property: $\mathbb{E}[\hat{\nabla}_{\text{PAFT}}] = \mathbb{E}[\hat{\nabla}_{\text{GARL}}]$. \square

Proposition E.4 (GARL has strictly lower variance than PAFT). *Under the same setup, $\text{Var}(\hat{\nabla}_{\text{PAFT}}) \geq \text{Var}(\hat{\nabla}_{\text{GARL}})$, with equality only when $\text{Var}(\hat{\nabla}_{\text{PAFT}} | \text{pool}) = 0$ almost surely.*

Proof. By Proposition E.3, $\mathbb{E}[\hat{\nabla}_{\text{PAFT}} | \text{pool}] = \hat{\nabla}_{\text{GARL}}$. The law of total variance gives

$$\begin{aligned} \text{Var}(\hat{\nabla}_{\text{PAFT}}) &= \text{Var}(\mathbb{E}[\hat{\nabla}_{\text{PAFT}} | \text{pool}]) + \mathbb{E}[\text{Var}(\hat{\nabla}_{\text{PAFT}} | \text{pool})] \\ &= \text{Var}(\hat{\nabla}_{\text{GARL}}) + \underbrace{\mathbb{E}[\text{Var}(\hat{\nabla}_{\text{PAFT}} | \text{pool})]}_{\geq 0}, \end{aligned}$$

with equality iff $\text{Var}(\hat{\nabla}_{\text{PAFT}} | \text{pool}) = 0$ a.s. This holds when, for each pool realization, all resampled trajectories produce the same gradient—e.g., when a single trajectory dominates the importance weights. In the non-degenerate case, the inequality is strict. \square

E.4 Pseudocode for GARL and PAFT

Algorithm 1 GARL: per-example J_Q gradient with RLOO control variate. *Numerical stability:* $w_m = \prod_t p_\theta(y_t^* | \cdot)$ underflows for long \mathbf{y}^* in linear-space arithmetic, so $w_m, \bar{w}_M, \bar{w}_{-m}$, and c_m should be computed in log-space (e.g., LogSumExp); the pathwise term $\nabla_\theta w_m / (\bar{w}_M)^q$ should be implemented as $\frac{w_m}{(\bar{w}_M)^q} \nabla_\theta \log p_\theta(\mathbf{y}^* | \mathbf{x}^*, \mathbf{z}^{(m)})$ (log-derivative trick), with the coefficient computed in log-space before being applied to the log-probability gradient.

Require: Example $(\mathbf{x}^*, \mathbf{y}^*)$, interpolation parameter $q \in [0, 1]$, number of latent samples $M \geq 2$ (for the leave-one-out baseline)

- 1: Sample latent trajectories $\mathbf{z}^{(1)}, \dots, \mathbf{z}^{(M)} \sim p_\theta(\cdot | \mathbf{x}^*)$
- 2: **for** $m = 1, \dots, M$ **do**
- 3: $w_m \leftarrow p_\theta(\mathbf{y}^* | \mathbf{x}^*, \mathbf{z}^{(m)})$ ▷ likelihood weight
- 4: $\nabla_\theta w_m \leftarrow \nabla_\theta p_\theta(\mathbf{y}^* | \mathbf{x}^*, \mathbf{z}^{(m)})$ ▷ pathwise gradient of output likelihood
- 5: **end for**
- 6: $\bar{w}_M \leftarrow \frac{1}{M} \sum_{m=1}^M w_m$ ▷ batch mean (estimates P_θ)
- 7: **for** $m = 1, \dots, M$ **do**
- 8: $\bar{w}_{-m} \leftarrow \frac{1}{M-1} \sum_{j \neq m} w_j$ ▷ leave-one-out mean
- 9: $c_m \leftarrow \frac{w_m}{(\bar{w}_M)^q} - (\bar{w}_{-m})^{1-q}$ ▷ centered weight (RLOO baseline)
- 10: $\hat{g}_m \leftarrow -c_m \nabla_\theta \log p_\theta(\mathbf{z}^{(m)} | \mathbf{x}^*) - \frac{\nabla_\theta w_m}{(\bar{w}_M)^q}$ ▷ score-function + pathwise terms
- 11: **end for**
- 12: **return** $\hat{g} \leftarrow \frac{1}{M^q} \cdot \frac{1}{M} \sum_{m=1}^M \hat{g}_m$ ▷ per-example gradient estimate, rescaled by $1/M^q$ to bound per-sample advantage uniformly in q

Algorithm 2 PAFT: per-example J_Q gradient via importance resampling. *Numerical stability:* the resampling step should be implemented with a categorical distribution parameterized by log-weights, e.g., Categorical(logits = $[\log w_1, \dots, \log w_M]$), to avoid division-by-zero when all w_m underflow.

Require: Example $(\mathbf{x}^*, \mathbf{y}^*)$, interpolation parameter $q \in [0, 1]$, prior samples M , resampled trajectories K

- 1: Sample latent trajectories $\mathbf{z}^{(1)}, \dots, \mathbf{z}^{(M)} \sim p_\theta(\cdot | \mathbf{x}^*)$
- 2: **for** $m = 1, \dots, M$ **do**
- 3: $w_m \leftarrow p_\theta(\mathbf{y}^* | \mathbf{x}^*, \mathbf{z}^{(m)})$ ▷ likelihood weight (same as GARL)
- 4: **end for**
- 5: $\bar{w}_M \leftarrow \frac{1}{M} \sum_{m=1}^M w_m$ ▷ batch mean (estimates P_θ)
- 6: Resample indices $r_1, \dots, r_K \sim \text{Categorical}(w_1 / \sum_j w_j, \dots, w_M / \sum_j w_j)$
- 7: $\hat{g} \leftarrow -\frac{(\bar{w}_M)^{1-q}}{M^q K} \sum_{k=1}^K \nabla_\theta \log p_\theta(\mathbf{z}^{(r_k)}, \mathbf{y}^* | \mathbf{x}^*)$ ▷ attenuated SFT on coherent rationales, rescaled by $1/M^q$ for advantage bounding
- 8: **return** \hat{g} ▷ rescaled per-example gradient estimate (matching Alg. 1’s $1/M^q$ convention)

F Additional Experimental Details

Subset construction. We sample subsets from Huggingface datasets: FinQA from dreamerdeo/finqa, HotPotQA from hotpotqa/hotpot_qa, and MuSiQue from bdsaglam/musique. We construct training, validation, and test subsets by retaining instances whose pre-tokenization input length (in characters) falls below predefined caps. The caps are 8000, 4000, and 10000 characters for FinQA, HotPotQA, and MuSiQue respectively. The resulting train/val/test subset sizes are 6145/872/1132, 9067/342/343, and 9985/579/445 for the 3 datasets respectively.

Training setup. We do not apply KL regularization to a reference policy, following the VeriFree setup [Zhou et al., 2026]; Liu et al. [2025] found KL does not improve performance in this regime. Per-rationale token budgets force the thinking-end token ($\langle /think \rangle$ for Qwen) once the budget is exhausted [Muennighoff et al., 2025]; see *Generation lengths* below. We use the AdamW optimizer [Loshchilov and Hutter, 2019] for all experiments. Training batch size is 64, and learning rate is set to 5×10^{-7} for Qwen 3 0.6B (higher learning rate was unstable in preliminary experiments), and 1×10^{-6} for Qwen 3 8B experiments respectively. We train for 2 epochs for all datasets, with a constant learning rate (no warmup or decay). Rollouts during training use temperature 1.0 (with top- k /top- p sampling disabled).

Model selection. We evaluate on the validation sets every 50 steps, and also at the end of training. We select the checkpoint that performs best on the $m@16$ metric.

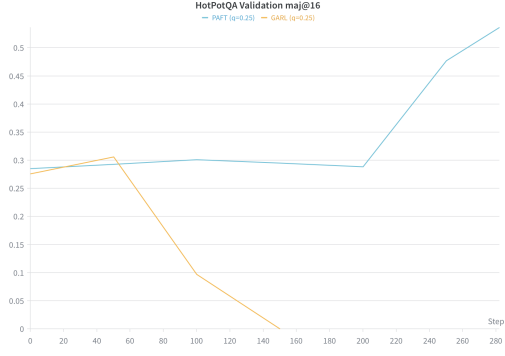
Generation lengths. We cap the maximum generation lengths to be 4096 for FinQA, 3072 for HotPotQA, and 2048 for MuSiQue. In addition, we allocate 128 tokens at the end of generation for the answer.

Compute. We conduct experiments on an 8-GPU (NVIDIA A100 80Gb) machine. A single training step takes approximately 3 minutes.

G Additional empirical figures



(a) Cold-start FinQA: maximum amplified advantage c_m/M^q vs. step, where $c_m = w_m/(\bar{w}_M)^q - (\bar{w}_{-m})^{1-q}$ is the centered weight from Equation (17) (bounded in $[-1, 1]$ after dividing by M^q). $q=1$ escapes immediately ($\Theta(\log(1/p_0))$); $q=0.75$ escapes sharply around step 35; $q \leq 0.5$ remain flat — qualitatively consistent with Theorem 3.1.



(b) Warm-start HotPotQA validation $m@16$ at $q=0.25$: GARS peaks at step 50 (30.6) and collapses to zero by step 100; PAFT remains stable, peaking at 53.6 (cf. test $m@16$ of 47.0 in Table 2).

Figure 2: GARS behavior across regimes. (a) Cold-start dynamics on FinQA: high q enables escape; despite faster escape, $q=1$ has lower test accuracy than $q=0.75$ (Table 1), consistent with the $O(q/MP_\theta^q)$ ratio-estimator bias of Theorem 4.1 degrading gradient quality. (b) Warm-start validation curves at fixed $q=0.25$ isolate the estimator (prior-sampled, all- M vs. posterior-resampled).

H Future directions

Multi-example dynamics. Our convergence analysis considers a single example. Across examples, the dynamics on each p_i involve the kernel $K_{ij} = \nabla_{\theta} P_i \cdot \nabla_{\theta} P_j$. Its interplay with the q -dependent weighting P_j^{-q} (potentially via NTK theory) could characterize how dataset-level coverage emerges from gradient-level amplification.

Annealing and richer posterior sampling. Principled schedule design adaptive to the current P_{θ} , and automatic switching between GARL and PAFT, remain open. PAFT’s importance resampling from the prior pool fails at cold start (vanishing attenuation and particle degeneracy); learned proposals, MCMC, or infilling models conditioned on both \mathbf{x}^* and \mathbf{y}^* could extend PAFT to lower- P_{θ} regimes.

Broader Impacts

This work is methodological: we propose a loss family and corresponding gradient estimators for training reasoning language models, using publicly available checkpoints (Qwen 3) and benchmarks (FinQA, HotPotQA, MuSiQue); no new pre-trained models or datasets are released. The J_Q continuum and its estimators (GARL, PAFT) enable post-training without annotated rationales, lowering the data bar for adapting reasoning models to specialized domains, low-resource languages, or settings where rationale annotations are expensive or unavailable. As with any post-training improvement, our methods could in principle be applied to fine-tune models for harmful applications; the same dual-use considerations apply to any RL-based post-training method (*e.g.*, GRPO, RLHF), and our contributions at the level of the training objective remain compatible with existing safety-relevant training procedures.